RENEWABLE POLYOL OBTAINED BY MICROWAVE-ASSISTED ALCOHOLYSIS OF EPOXIDIZED SOYBEAN OIL: PREPARATION, THERMAL PROPERTIES AND RELAXATION PROCESS

Diana Favero[a], Victória Marcon[a], Thiago Barcellos[a], Clara M. Gómez[b], Maria J. Sanchis[c], Marta Carsí[d], Carlos A. Figueroa[a], Otávio Bianchi[a]

[a]Programa de Pós-graduação em Engenharia e Ciência dos Materiais – PGMAT, Universidade de Caxias do Sul, Getúlio Vargas, 1130 – CEP 95070-560 Caxias do Sul, RS, Brasil.

[b]Instituto de Ciencia de los Materiales, Universidad de Valencia, 46980 Paterna, Valencia, Spain.

[c]Department of Applied Thermodynamics, Institute of Electric Technology, Universitat Politècnica de València, Valencia, Spain.

[d]Department of Applied Thermodynamics, Instituto de Automática e Informática Industrial, Universitat Politècnica de Valencia, 46022 Valencia, Spain.

Correspondence to: O. Bianchi +5554-98403-0958 (E-mail: *otavio.bianchi@gmail.com*); D. Favero +5554-99139-4191 (E-mail: *difavero@yahoo.com.br*)

Abstract: The soybean oil polyol (SOP) use as feedstock in the polyurethane industry has been recently emphasized due to its excellent resistance to hydrolysis, which is also applicable in coatings and thermal insulation. In this article, the SOP was obtained by a very fast microwave-assisted alcoholysis of epoxidized soybean oil (ESO). The preparation method, thermal properties, and relaxation process were evaluated. High yields as opening and consumption epoxy group and selectivity of 99.8 mol%, 98.5 mol%, and 71.2 mol% were obtained. Through titrations, nuclear magnetic resonance and gel permeation chromatography were identified parameters as 0.32 mg KOH.g^{-1} acid number, 190 mg KOH·g^{-1} hydroxyl number, 150 mg KOH·g^{-1} saponification index, 0.17 wt.% water content, 1463 g·mol^{-1} molecular weight, 4.98 average functionality, 2.4x10^{-5} mPa·s^{-1} viscosity at 333K and 1.00 g·cm^{-3} density. The dielectric relaxation spectroscopy allowed identifying the α-relaxation process with a 193.5K glass transition (T_g), 63.2 fragility index and 234.1 kJ mol^{-1} activation energy associated with T_g from the dynamic fragility index. The ionic conductivity temperature dependence on SOP obeys Arrhenius behavior. In summary, the SOP structure and thermal relaxation parameters determination are fundamental for the understanding of the structure-properties relationship of renewable polyurethanes.

Keywords: soybean oil polyol, microwave-assisted alcoholysis, thermal properties, dielectric relaxation spectroscopy.

1. Introduction

Vegetable oils like soybean, sunflower, cotton, and castor oil are excellent raw materials for the development of monomers in polymer synthesis [1, 2]. Soybean oil (SO) has been widely used in the chemical industry, due to its availability and low cost, to produce numerous substances through chemical reactions e.g., epoxidation, oxidation, ozonolysis, catalytic hydrogenation, and glycerolysis [1, 3]. In addition, the agriculture-based triglycerides are considered to be "green" raw materials. Brazil is the world´s second-leading soybean producer and therefore the soybean oil (SO) is widely available. The triglycerides of SO contain saturated and unsaturated fatty acids. The proportion of unsaturated fatty acids is greater than 80 wt.% in this oil. This turns into an unsaturation degree (iodine number) with a value between 120-141 g of I_2/100g. However, SO molecules require specific chemical reactions to generate hydroxyl groups at the position of double bonds. Chemical reactions in SO can also be used for obtaining products such as biodiesel, polyols, and surfactants. Among the existing chemical processes for the polyols production, we can mention a consolidated and widely used method as the epoxidation and subsequently epoxy ring opening. This process is usually carried out in two stages. The first one corresponds to the epoxidation of the double bonds of vegetable oil with hydrogen peroxide or acid performic and a carboxylic acid to form peracetic or performic acid in situ. The second stage is the epoxy ring opening reaction to form hydroxyl groups [4]. In this approach, it is possible to obtain polyols with hydroxyl index in the range of 180-230 mg KOH/g, a low acid index with high functionality (around 3-12). The synthesized polyurethane materials (PU) from soybean oil polyol (SOP) show high crosslink density, good mechanical properties such as high tensile strength, hydrolysis resistance, and good thermal stability [4, 5].

SOP becomes a total or a partial alternative to the replacement of petroleum-derived polyols. Alcoholysis reaction conducted in an oil bath (based on convection and conduction mechanisms) requires reaction times around 8-12 h, including an epoxy ring opening degree between 70-95 wt.% [6, 7]. The alternative route as the use of dielectric heating as a microwave-assisted reaction is considered an interesting technique for polyol or polymer synthesis and nanomaterials preparation [4, 8]. In this approach, a number of advantages can be observed: the reduction of time/temperature required for its synthesis. Prociak et al. [9] reported the use of microwave-assisted heating for obtaining SOP with hydroxyl values of 114−196 mg $KOH.g^{-1}$ using an acid alcoholysis reaction. They observed a 75 % reduction in the reaction time when compared with oil bath process conditions. The popularity of microwave-assisted chemistry is not surprising considering that this method dramatically increases the yield and decreases the reaction times. Microwave radiation acts directly entire reaction medium on the molecules, leading to a rapid rise of the temperature. Therefore, localized superheating of the sample can be produced by rotating or dipolar ionic conductivity [8, 10].

The interactions between the reactants and the electromagnetic field are related by increasing the selectivity and reaction rate leading to the thermal and specific (non-thermal) effects of microwave radiation [10]. Nonetheless, for the efficiency of the microwave heating, the substance needs to have a suitable dipole moment to be active to the electromagnetic field effect [10]. Lin et.al [11] studied the relationship between melting peak and the number-average functionality of hydroxyl in SOPs by differential scanning calorimetry (DSC). They found a direct relation of epoxidation time (6−28 h) with the average functionality and melting temperatures of the polyols. Thus, greater functionality in polyols causes the melting peak to shift to higher temperatures due to oligomerization. Although the SOP shows great prominence in scientific and industrial research, its thermal behavior characterized by its glass transition (T_g) is still unclear. In general, published results on the glass transition or second-order transitions of polyols from vegetable oils lead to confusing conclusions [12]. Differential scanning calorimetry (DSC) shows restrictions to identify the Tg temperature of SOP since other functionalities such as olefins and ester linkages with glycerol exhibit melting peaks with relatively broad transitions at the same range of temperature values. So, usually, the T_g of SOP is determined from the tan δ in Dynamic Mechanical Thermal Analysis analysis (DMTA) of soy-based polyurethanes. Nevertheless, the Tg temperature determination pure SOP and of soy-based PUs is crucial to understand the morphology, phase separation degree, microphase composition and dynamic-mechanical properties for future applications of this renewable PUs.

Minoguchi et al. [13] studied the dielectric relaxation processes of different polyols. Dielectric measurements were performed in sorbitol, xylitol, and sorbitol-xylitol mixtures in the supercooled liquid state in a wide frequency range at temperatures near and above the T_g. In dielectric relaxation spectroscopy (DRS) spectra, two dipolar relaxations were observed. A primary α-relaxation process related to the T_g phenomenon, and a secondary β-process dipolar relaxation. The β-relaxation is related to the hydrogen bonds among molecules, which are strongly bonded to molecules and behave like bound water, and is very similar for all the polyols including glycerol. The glycerol β-process showed very small and strong relaxation. It presents a very low temperature. In this way, the thermal behavior represented by T_g and β-relaxation process, that are associated with the conformational crankshaft motion of the SOP main chain [14] were discussed. The relaxation process is possible only in the amorphous region as concluded from the low-temperature tan δ peaks in dielectric measurements near -393K [14]. Then, the dielectric behavior represents a powerful tool for investigation the polyol molecular dynamics in a frequency and temperature wide range.

In this paper, we report the synthesis and physicochemical characterization of soybean polyol (SOP) which plays a key role in the polyurethanes synthesis with tunable characteristics. Although, for vegetable oils polyols the production process is already well established in the literature [5, 7, 15]

some advantages can be obtained by means of the ESO microwave-assisted alcoholysis reaction as the reduction in preparation time. It does not require the catalysts using, it is a cleaner process. The results achieved so far represent a scientific advance compared to previous work [4, 7, 16]. The SO chemical modifications each reaction step were measured by nuclear magnetic resonance spectroscopy (NMR), titrations, density, Fourier transform infrared spectroscopy (ATR-FTIR). The SOP molecular dynamic characterization by differential scanning calorimeter (DSC) and dielectric relaxation spectroscopy (DRS) allows determining relevant processing parameters as the glass transition temperature (T_g), the activation energy associated with the relaxation dynamics of the chains at T_g and the dynamic fragility index. Thus, we introduce some understandings about the microwave-assisted soybean polyol preparation and in its physicochemical behavior, it is fundamental in the polyurethanes synthesis with tunable characteristics.

2. Experimental section

2.1 Materials

Commercially refined SO (Primor, Bunge Alimentos S.A, Brazil) with an 0.80 ± 0.11 mg KOH·g^{-1} acid number and 5.00 mol double bonds/mol of triglyceride molecules (^{1}H NMR $CDCl_3$ 25ºC), 0.90 ± 0.01 g·cm^{-3}density, and an 936.0 g·mol^{-1} average molecular weight (GPC) was used. The following raw materials were used to obtain the ESO and SOP: 99.8 wt.% glacial acetic acid, (AA; CAS number 64-19-7) purchased to Neon, 30 wt.% aqueous solution hydrogen peroxide (H_2O_2; CAS number 7722-84-1), sulfuric acid (H_2SO_4; CAS number 7664-93-9), calcium hydroxide (CAS number 1305-62-0) and diethylene glycol (DEG; CAS number 111-46-6) were purchased from Dynamic.

2.2 Synthesis of renewable soybean Polyol

Step 1: Epoxidation of soybean oil (ESO)

This procedure was followed according to Milchert et al. [17] soybean oil 300.0 g, hydrogen peroxide 110.80g, acetic acid 23.1 g (1:9.5:1.12 mol/mol molar ratio) and catalyst H_2SO_4 (0.5 wt.% in relation to the total reaction mixture) 2.16 g were added to 1 L round-bottomed flask three-necked, equipped with a thermometer, mechanical stirrer, reflux condenser, dropping funnel, and heating mantle. The mixture was stirred at 500 rpm for 4 h at 333 K. And then, after the epoxidation reaction the organic layer was separated at 298 K, which contains water and organic acids that can cause the epoxy ring decomposition. Its mixture with ESO causes the phases separation due to the solubility difference. The mixture was washed with distilled water and 20 wt.% calcium hydroxide (5x450 cm^3

water per 0.16 mol of ESO) to removed acidity [17]. The remaining water was removed by centrifugation and vacuum distillation.

Step 2: Microwave-assisted alcoholysis reactions

The epoxy ring-opening reaction was catalyzed in acid medium by alcoholysis reaction an adapted microwave reactor (2.45 GHz frequency and 750 W microwave power) according to a procedure described in the literature [8]. ESO 150 g and diethylene glycol (DEG) 19.6 g (0.315:0.16 mol/mol molar ratio) [4] were added to 250mL bottomed flask quartz square equipped with a magnetic stirrer bar without using a catalyst. Thus, the reactions came out by using magnetron cycles (on/off) to avoid overheating [8]. The alcoholysis reaction was carried out at 300 and 600 s samples time (t) in 20, 40 and 50 s cycles with the magnetron on (c_{on}), and 10, 5 and 1 s with the magnetron off (c_{off}). In summary, this will be shown following way: ($t/c_{on}/c_{off}$) s.

2.3 Chemical Characterization

The number-average molecular weight (M_n) was determined by means of gel permeation chromatography (GPC). The GPC experiments were performed on a Viscotek VE2001 chromatograph coupled to a Viscotek TDA302 detector at 318 K, using THF as a solvent with a 10 $mg{\cdot}mL^{-1}$ sample concentration and 1.0 $mL{\cdot}min^{-1}$ mobile phase flow rate. Polystyrene standards were used to plot the calibration curve.

The soybean oils and polyol thermal transitions were determined by differential scanning calorimetry (DSC) using a Netzsch DSC 204 Phoenix with 9-10 mg of the sample under nitrogen atmosphere (50 $mL.min^{-1}$). The melting temperature and enthalpy were calibrated with indium, tin, bismuth, and zinc standard patrons. The samples were analyzed from 93 to 473K at a 20 $K{\cdot}min^{-1}$ heating rate.

The viscosity was determined with a Brookfield viscometer LVDV-II+ coupled to a thermostatic bath at 333K, thus allowing to measure the viscosity of the samples with spindle S61 (19.00mm external diameter cylinder).

The acid value, hydroxyl value, saponification value and water content of the polyol were determined by titration analysis according to the American Society for Testing and Materials ASTM-D1639-9002 [18], ASTM-D5558 – 95 [19], ASTM-D4274 [20] and ASTM-E203-01 [21]. The water content (ASTM E 203-01) was measured by Karl-Fischer titration in a DMS Titrino Metrohm 716 automatic titration.

The chemical groups formed during epoxidation and alcoholysis reactions were monitored by spectroscopy analysis (FTIR and NMR). ATR-FTIR analysis was carried out with a Perkin-Elmer

Spectrum 400 spectrometer in attenuated total reflection (ATR; diamond crystal at 45°) mode. The spectra were obtained by averaging 32 scans over the 4000–450 cm^{-1} region with a 2 cm^{-1} resolution.

The epoxidation degree, the triglycerides double bonds (CD), epoxy ring number for TGD (E), epoxy ring opening consumption, and the selectivity were investigated by hydrogen nuclear magnetic resonance (^{1}H NMR) [22, 23]. The primary and secondary hydroxyl groups relative content was evaluated by carbon nuclear magnetic resonance (^{13}C NMR) [24].

The ^{1}H and ^{13}C NMR analyses were carried out on a Bruker Fourier 300 spectrometer at 300.18 MHz and 75.48 MHZ, respectively. The ^{1}H NMR spectra were acquired using sample 10 mg $CDCl_3$ dissolved into 600 µL at 292.3 K, 32 scans, a 1 s relaxation delay, 3.25 s acquisition time and 90° pulse width. The ^{13}C NMR spectra were acquired using sample 40 mg, $CDCl_3$ dissolved into 600 µL at 292.3 K, 4.096 scans, a 1 s relaxation delay, 1.342 s acquisition time and 13.2°pulse width. Thus, the tetramethylsilane (TMS) signal shown in CDCl3 was used as a reference for chemical shifts. The doublet of doublets at 4.10 and 4.35 ppm were used as the internal standard for quantification, which are associated with the protons at positions C (1) and C (2) of glycerol.

The dielectric relaxation spectroscopy measurements (DRS) in the frequency range from 10^{-2} Hz to 10^{6} Hz were performed using a Broadband Dielectric Spectrometer (Novocontrol BDS 40 spectrometer based on an Alpha impedance analyzer, Novocontrol Technologies GmbH) with automatic temperature control (Quatro Cryosystem, Novocontrol Technologies GmbH). The measurements were conducted using a three-electrode cylindrical sample holder (BDS 1307, Novocontrol) that corrects results due to thermal expansion of samples, prevents liquid leakage and minimizes the fringing fields effects by using a guard electrode. In order to improve the accuracy, calibration of the sample cell was performed using standard samples. The calibration details are referred in the manual of Cylindrical Liquid Sample Cell BDS 1307, Novocontrol. [25] Accordingly, the empty cell and stray capacities were 1.095 pF and 2.269 pF respectively. The sample height was 5 mm, inner and outer electrode diameters were 20 mm and 26.5 mm respectively. We have used standard experimental setting recommended by Novocontrol. The applied voltage was 1 V (the resultant field strength remains in the linear regime). The samples were cooled down up to 143K and then gradually heated and measured with a temperature step of 5 K up to 313 K. Isothermal frequency scans were acquired with temperature stability of ± 0.3 K in a N_2 flow Quattro cryostat (Novocontrol Technologies). The sample was in a nitrogen flux during all measurements.

3. Results and discussion

The epoxidation reaction is an important step to obtain polyol from renewable sources. In this step, the peracetic acid (PAA) was formed in situ from the reaction between H_2O_2 and CH_3COOH. Therefore, PAA migrated to the oil phase and spontaneously reacted with double bonds of SO forming the epoxy ring [7, 17]. The H_2O_2 was added dropwise increasing the temperature from 333 K to 363 K. Then, the medium reaction was cooled and maintained at 333 K, in order to avoid epoxy ring opening and possible secondary reactions formation. In this step, the epoxidized soybean oil (ESO) was obtained with a 28.70 mg $KOH \cdot g^{-1}$ acid value (AI) (see Table 1). Then, the ESO was neutralized with an 20wt.% $Ca(OH)_2$ aqueous solution and it was gotten an 5 $mg.KOH.g^{-1}$ acid value, to avoid secondary reactions during microwave-assisted alcoholysis.

In Figure 1 are shown the FTIR spectra for SO, ESO and SOP obtained under time reaction of 5 min. (300 s) using the magneton on 20 s and off 10 s (300/20/10) s. Triglycerides bands typical were observed in all samples [1, 7]. Carbonyl ester group at 1740 cm^{-1}, aliphatic hydrocarbons groups at 1463, 2922 and 2825 cm^{-1}, bending vibrations of the $–CH_2$ at 722 cm^{-1} [2, 17] and (C=)C-H double bonds in the chain at 3010 cm^{-1} were observed [5, 7]. The ESO spectrum showed also two new absorption bands at 24 and 845 cm^{-1} that are epoxy rings characteristic [26]. In addition, a characteristic hydroxyl group (-OH) band at 3346 cm^{-1} was also observed. Hydroxyl band in SO indicated that the epoxy ring opens during epoxidation reaction, confirmed by titration analysis (Table 1). The SOP spectrum showed a new absorption band of ether group stretching vibration (C-O-C) in the region 1053 cm^{-1} and a more intense hydroxyl band when compared to ESO at 3600 and 3300 cm^{-1} [4].

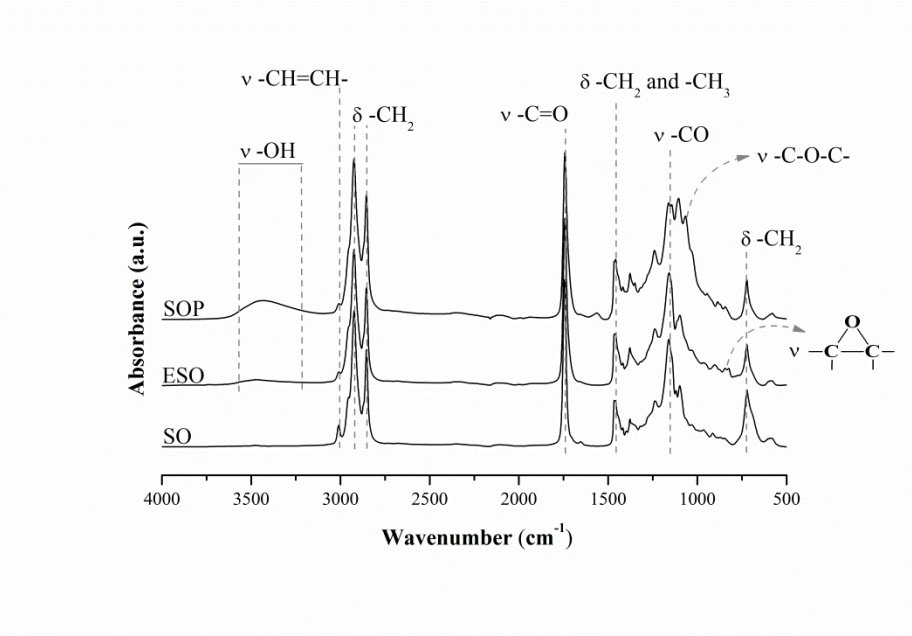

Figure 1 FTIR spectra of the soybean oil (SO), epoxidized soybean oil (ESO) and soybean oil polyol (SOP) obtained under the condition of microwave-assisted alcoholysis reaction of 300/20/10 s.

The ^1H NMR spectra of SO, ESO and SOP are shown in Figure 2. All the samples depict the

same characteristic spectra at δ 5.39 ppm (A) all unsaturated fatty acids (-C<u>H</u>=C<u>H</u>-) [27], δ 5.20 ppm (B) glycerol β-position (-C<u>H</u>-O-COR), δ 4.19 ppm glycerol α-position (-C<u>H</u>$_2$-O-COR), δ 2.76 ppm (D) bis-allylic protons (-CH=CH-C<u>H</u>$_2$-CH=CH-), δ 2.29 ppm (E) all acyl chains (-C<u>H</u>$_2$-COOH), δ 2.0 ppm (F) allylic protons of all unsaturated fatty acids (-C<u>H</u>$_2$-CH=CH-), δ 1.6 ppm (G) all acyl chains (-C<u>H</u>$_2$-CH$_2$-COOH), δ 0.85 ppm (H) all acyl chains except for linolenic (-CH$_2$-CH$_2$-CH$_2$-C<u>H</u>$_3$) and δ 1.27 ppm (I) all acyl chains (-(C<u>H</u>$_2$)n-) [27]. The SO spectrum reveals the formation of 5 double bonds (C=)C-H for each triacylglycerol. The ESO spectrum indicates that the unsaturated fatty acids (A) were converted into epoxy groups classified as monoepoxides and diepoxides (J) with signals appearing at δ 2.9-3.0 ppm (-C<u>H</u>OCH-CH$_2$- CHOC<u>H</u>-) and δ 3.09-3.16 ppm (-CHOC<u>H</u>-CH$_2$-C<u>H</u>OCH-), as well as, at δ 1.45-1.60 ppm methylene protons adjacent epoxy group (-CH$_2$-C<u>H</u>$_2$ -CHOCH-) and at 2.0 ppm methylene alpha group to acyl group (CH$_2$-C<u>H</u>$_2$-C=O-O-) [27]. However, in the SOP spectrum, the signals at δ 3.40 -3.76 ppm (OH-CH$_2$-CH$_2$-O<u>H</u>) methylene hydrogens bonded, -CH$_2$-(O-CH$_2$-CH$_2$-O-C<u>H</u>$_2$-CH$_2$-OH) alpha-methylene group and (-CH$_2$-C<u>H</u>(OH)-C<u>H</u>(OH)-CH$_2$-) methine beta group [28], indicated the hydroxyl groups formation (L). Thus, the J region disappeared during the alcoholysis reaction, indicating that the monoepoxide and diepoxide rings were fully opened (see more details in Supplementary files/Table S1).

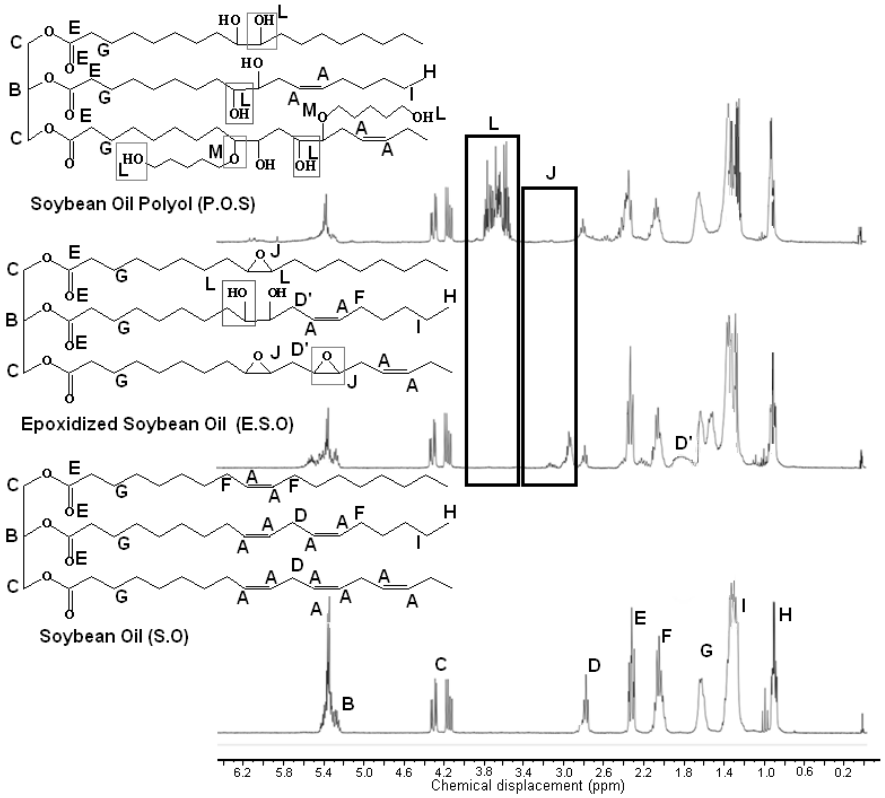

Figure 2 H[1] NMR spectra of the soybean oil (SO), epoxidized soybean oil (ESO) and soybean oil polyol (SOP) obtained under the condition of microwave-assisted alcoholysis reaction of 300/20/10 s.

Further structural evidence is shown in Figure 3 with complementary ^{13}C NMR spectra to SO, ESO and SOP (see more details in Supplementary files/Table S2). The ESO spectrum showed the monoepoxides and diepoxides opening during the epoxidation reaction followed by hydroxyl group formation at δ 60.0-89.9 ppm (L). SOP spectrum depicted hydroxyl groups formation (L) due to the alcoholysis reaction of the epoxy ring reacted with DEG. Total epoxy ring consumption was confirmed in the ^{1}H NMR spectrum. It also was evidenced at δ 70.0ppm (N) ether group formation (as 69.5 – 70.5 ppm enlarged region).

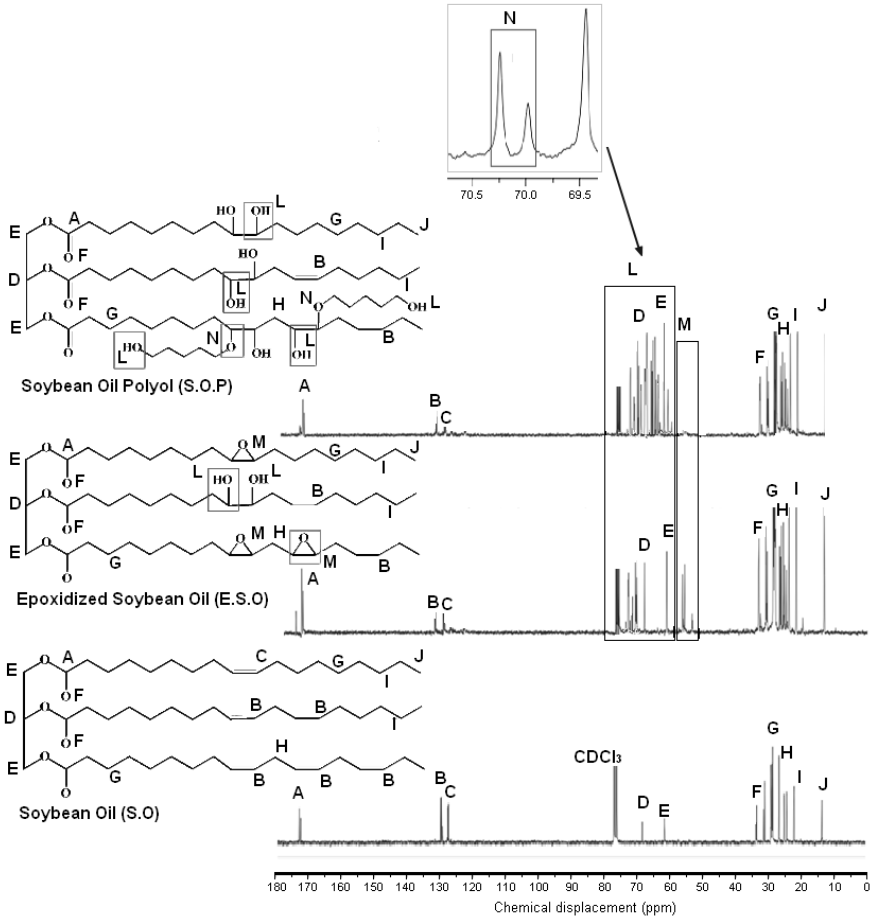

Figure 3 ^{13}C NMR spectra of the soybean oil (SO), epoxidized soybean oil (ESO) and soybean oil polyol (SOP) obtained under the condition of microwave-assisted alcoholysis reaction of 300/20/10 s.

All SOP production steps were characterized by acid index, saponification index, hydroxyl number, water contents, molar mass and average functionality, density and viscosity, as shown in Table 1. The viscosity values increase was observed in the SOP due to the hydroxyl groups formation [4]. In this way, all samples showed a Newtonian rheological behavior. During epoxidation reactions with the situ formation of peracetic acid, the epoxide ring may open. This was followed by spectroscopic analyzes (NMR and FTIR) and titration (see Table 1) in this work. Dworakowska et al.

[4] reported the polyol synthesis from rapeseed oil using microwave-assisted acid alcoholysis reactions. This process was performed in the range of 273 – 378K during 1 h (200 – 300 W) and yielded a polyol with 196 mg KOH·g^{-1} hydroxyl number. In this work, the potentiality of the proposed method was evidenced. We have achieved a significant reduction in time, requiring only an alcoholysis reaction time of only 5 minutes. The SOP produced has 98.5 mol % selectivity epoxy ring opening (Table 2) and 190 mg KOH·g^{-1} hydroxyl number. There was not the soap formation and 0.17 wt.% water content is conform to the commercial polyol standard. This polyol SOYOL ™ R3-170 was synthesized from SO and has a water content less than 0.20 wt.% available by Urethane Soy Systems Company [29]. Furthermore, PU synthesis with the use of this polyol will give an oligomerization side reactions low possibility due to the 0.32 mg KOH·g^{-1} free fatty acids formation. Short-chain polyols (250 < 1000 g.mol^{-1}) and high functionality (3-12) produce rigid chains with high cross-linking properties and can be used in the synthesis of high-performance foams, coatings, and paints [30]. Other authors have obtained results similar to those got in the present study [4, 7, 26], but using much longer reaction times.

Table 1 Titrations, GPC, density and viscosity analysis of the soybean oil (SO), epoxidized soybean oil (ESO) and soybean oil poliol (SOP).

Properties	SO	ESO	SOP
Acid index (mg KOH·g^{-1})	0.80	28.70	0.32
Saponification index (mg KOH·g^{-1})	146	149	150
Hydroxyl number (mg KOH·g^{-1})	0.20	53	190
Water content (wt %)	—	—	0.17
Density (g·cm^{-3})	0.90	0.97	1.00
Molecular weight (g·mol^{-1})	936	1125	1463
Average functionality	0	1.12	4.98
Viscosity at 333K (mPa·s^{-1})	1.7x10^{-6}	1.9x10^{-6}	2.4x10^{-5}

During the alcoholysis reaction, there was the epoxy ring opening on the less substituted carbon due to their lower steric effect. Thus, the less the steric hindrance, the greater the preference for the nucleophilic attack. However, the epoxy ring is not fully consumed for hydroxyl group formation due to the oligomerization side reactions from SO [29]. Regarding the reaction time effect, according to the analyses carried out for long reaction times, the degradation of the SOP is promoted. Thus, under (600/40/05) s, (600/50/01) s, 600/40/05) s, and (600/50/01) s the reaction conditions produced a strong darkening of the polyol from yellow to brown. After optimization of the reaction conditions, the best condition of microwave-assisted alcoholysis reaction was obtained after only 5 min. (300 s) using the magnetron on 20 s and off 10 s (300/20/10) s. The subsequent analyses were carried out using the polyol obtained under these conditions of microwave-assisted alcoholysis. The microwave-assisted

heating use generates a localized heat, rapid and uniform during the alcoholysis reaction [8] inducing a faster conversion of the epoxy ring opening. The local temperature reached, in the range of 388 – 463K, did not generate degradation being obtained ER and E values 99.8 mol% and 98.5 mol%, respectively. According to the literature, the thermal degradation onset of vegetable oils starts at temperatures above 493K [31]. Polyol degradation is caused by long exposure at convective high temperature (above 493K) and not by the 2.45 GHz radiation energy which is equivalent to 1 J·mol^{-1} [29]. The DEG use in the microwave-assisted alcoholysis is appropriate due to their high value of tan δ (= 1.350), which favors speed up the epoxy ring opening reaction by polarization mechanism [10]. Table 2 shows the obtained results by using the method proposed by Campanella et al. [23] for the opening (ER) and consumption (E) of the epoxy ring. The microwave-assisted alcoholysis method has become more effective than reactions made in the oil bath. Thus, Allauddin et al. [7] synthesized the polyol from SO by conventional heating reactions made in oil bath with 10 h of the alcoholysis reaction and obtained an ER 95 mol%.

Table 2 Yield of soybean oil polyol (SOP) by ^{1}H NMR analysis. The opening (ER) and consumption (E) of the epoxide ring.

Samples Time/pulse on/off (s)	ER (mol%)	E (mol%)
300/20/10	99.8 ±0.1	98.5 ±0.1
300/40/05	90.1±0.3	43.2±0.1
300/50/01	89.0±0.4	43.1±0.2
600/20/05	86.0±0.1	46.6±0.4
600/20/10	86.0± 0.1	46.6± 0.3
600/40/05	84.4±0.5	46.7±0.1
600/50/01	81.9±0.1	44.3±0.3

The relative percentages of secondary to primary hydroxyl (X_S (R_2CH-OH) and X_P (RCH_2–OH)), were determined from ^{13}C NMR spectra, as proposed by Lebas et al. [24] by means the following Eq. 1:

$$\% X_p = \frac{A X_P}{A X_P + A X_S} \times 100 \quad (1)$$

Where $A X_P$ and $A X_S$ represent the primary hydroxyl group area ($A_{60.2-65.8ppm}$) and the secondary hydroxyl group area ($A_{65.9-89.9ppm}$), respectively. The $CDCl_3$ area ($A_{75.29-76.68ppm}$) was subtracted from the total to estimate secondary hydroxyl group area.

ESO spectrum presented 62.9 mol% and 37.1 mol% of secondary and primary hydroxyl groups, respectively. This result points in the primary hydroxyl group probably participated in inter- and intra-molecular bonds with the unreacted epoxy ring, with the consequent reduction of the primary

hydroxyls amount [32]. However, the SOP spectrum showed primary hydroxyl group 65.8 mol% due to epoxy ring reacted with DEG (see Table 3). The hydroxyl groups ratio directly influences the polyols reactivity during polyurethane polymerization. Probably, due to the steric effect imposed by the neighboring groups in secondary hydroxyl groups, the primary hydroxyl group react three times faster than the secondary ones [24, 33]. The epoxidation and alcoholysis reaction conversion was also estimated from the H^1 NMR spectra (Table 3). The signals associated with the protons of the *sn-1* and *sn-3* esterified glycerol (4.10-4.35 ppm) were used as internal standard signals because they remained constant during the hydrolysis reaction [27]. The signal at 0.88 ppm from methyl groups has been used for other authors as an internal standard for quantification [23, 28]. However, in oxidized oils, carbonyls and alkanes of shorter chain length are produced by the secondary bond backbone of the lipid oxidation intermediate products, especially at high temperature. The epoxidation reaction is a method widely used. We found in the literature different reaction times from 4 to 22 h with yields from 50 to75 mol% epoxidation degree (ED), 2.1−4.5 epoxy ring number/TGD (E), 65-92 mol% double bonds consumption (DC) [17, 22] and 80 mol% selectivity (S%) which is rarely higher [4], due to the epoxy ring opening reactions which are accompanied by oligomerization side reactions. Thus, in this, epoxidation reaction 4h is considered reasonable because obtained conversion was similar to those research previously published [4, 5, 7, 15].

Table 3 Properties to epoxidized soybean oil (ESO) and soybean oil polyol (SOP) by H^1 and ^{13}C NMR spectra quantification.

Properties (mol%)	ESO	SOP
Primary hydroxyl groups (X_P)	37.1 ± 1.1	65.8 ± 1.5
Secondary hydroxyl groups (X_s)	62.9 ± 0.9	34.2 ± 1.2
Epoxidation degree (EG)	60.2 ± 0.5	—
Epoxy ring number for TGD (E)	2.73 ± 0.4	—
Double bonds consumption (DC)	66.1 ± 1.2	70.5 ± 1.6
Selectivity (S)	—	71.6 ± 0.3

The DSC thermograms of the soybean oil (SO), soybean oil epoxidized (ESO) and soybean oil polyol (SOP) are shown in Figure 4. All samples exhibit a thermal transition at 162K associated with the group $-CH_2$ rotation motion that is associated with the amorphous regions attributed to the Schatzki mechanism [34]. As previously mentioned, the T_g identification by DSC is not guaranteed to owe to the wide melting peaks near the glass transition temperature. In the SO thermogram, there are two exothermic peaks at 195K and 212K attributed to the fatty acids crystallization and to the high density of double bonds, and three endothermic peaks lipid melting characteristics at 203K, 242K and 257K [35]. These last peaks are vegetable polyols typical and showed a polymorphic behavior due to the crystallization in the forms α, β', and β [36]. ESO shows a melting peak at ~265K, while in the SOP

was observed at ~270K due to the hydroxyl groups formation that contribute to intramolecular van der Waals interactions [15].

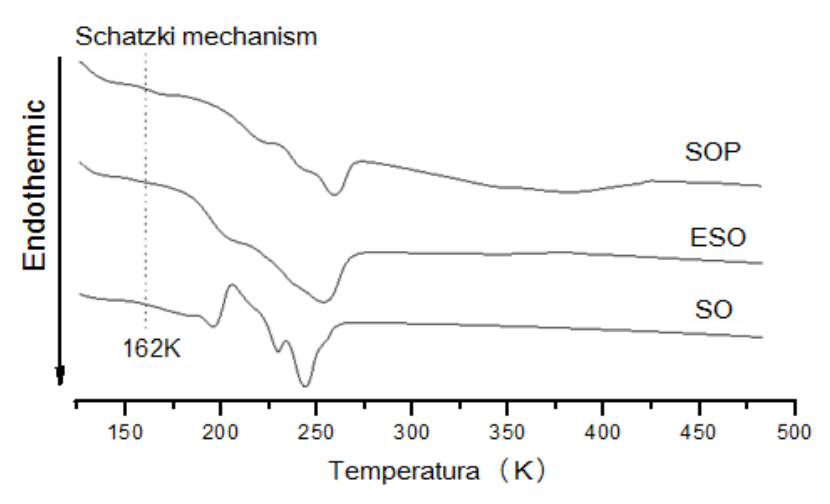

Figure 4 DSC thermograms of soybean oil (SO), epoxidized soybean oil (ESO) and soybean oil polyol (SOP).

Three dimensional (3D) representations of the real (□') and loss (□") components of the complex dielectric permittivity for SOP in the frequency range of 10^{-2} - 10^{6} Hz and temperature window of 143 - 313 K are presented in Figure 5. The dielectric permittivity (ε′) displays the same pattern for all isochrones. Thus, as usual, ε′ increases as temperature increases, reaching a plateau, corresponding to the relaxed dipoles, associated with the glass-rubber transition, or α relaxation process. For frequencies, the real component of the complex permittivity departs from the plateau in such a way that its value increases with increasing temperature, in the low-frequency region. Departure from the plateau shifts to higher frequency with increasing temperature. This increase is related to the electrode polarization (EP), coming from the charges accumulation at the electrode-polyol interface. On the other hand, the dielectric loss factor spectra present two relaxation zones. In the low-temperature zone, we can observe a very weakly defined secondary relaxation, labeled as β-processes, presumably associated with localized motions. In the high-temperature zone, the spectra present an ostensible α-relaxation attributed to the glass-rubber relaxation. As usual, conductive contributions overlap with the α-relaxation process in the low-frequency region. As the temperature is reduced from 323K to 133K, the broad peak moves towards lower frequencies and also increases its amplitude. This can be explained because as the temperature decreases the kinetic energy also decreases. Therefore, this generates lower random movements and thus a greater dipole orientation as the amplitude increases leading to higher dielectric constant values. At low temperatures, with increasing frequency, the dielectric constant (□') decreases significantly until reaching a plateau according to the Debye prediction equations [37].

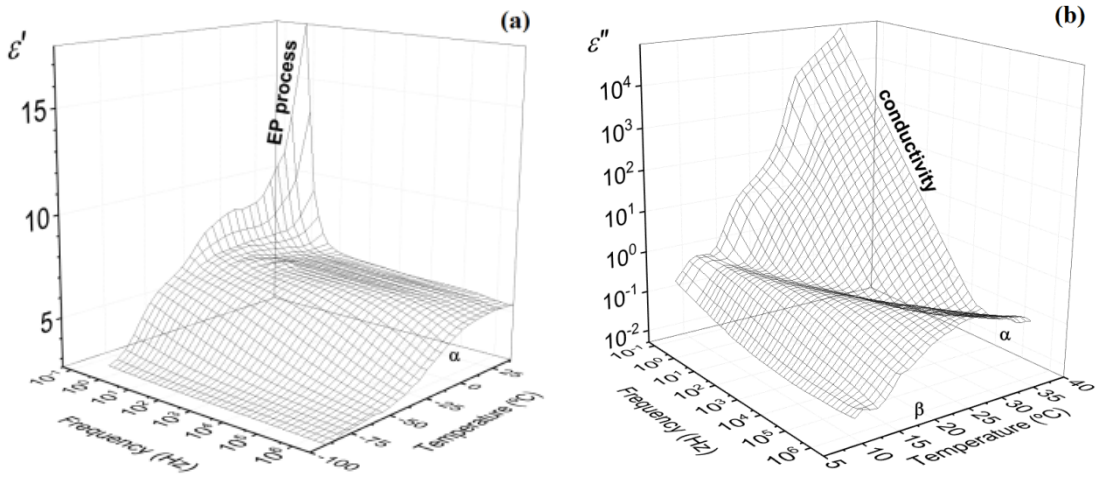

Figure 5 3D plots of the frequency and temperature dependence of the dielectric permittivity ε′ (a) and dielectric losses ε″ (b) for SOP in the temperature range of 313K to 143K at 5K steps and in frequency range of 10^{-2} – 10^{6} Hz.

In order to analyze the glass transition temperature, the dielectric spectrum analysis, in the frequency domain, was performed using the Havriliak-Negami (HN) empirical model, which correlates the complex permittivity (ε*) to the frequency by Eq. 2:

$$\varepsilon * (\omega) = \varepsilon_{\infty} + \frac{\varepsilon_0 - \varepsilon_{\infty}}{\left[1 + (j\omega\tau_0)^a\right]^b} \tag{2}$$

Where ω $(=2\pi f)$ is the angular frequency, ε_0 and ε_∞ are respectively the relaxed and unrelaxed permittivity ($\Delta\varepsilon = \varepsilon_0 - \varepsilon_\infty$ are the dielectric strength), τ_0 is the characteristic relaxation time and a and b $[0<a, ab\leq 1]$ are parameters determining the shape of the relaxation spectra and define the symmetrical and asymmetrical broadenings of the loss peak. The parameter a is related to the broadness of the relaxation curve (the higher the a parameter, the narrower the peak) and b parameter is related to the relaxation process symmetry. The splitting of equation (2) in real and imaginary parts gives:

$$\varepsilon'(\omega) = \varepsilon_{\infty} + r^{-\frac{b}{2}}(\varepsilon_0 - \varepsilon_{\infty}).\cos b\theta \tag{3}$$

$$\varepsilon''(\omega) = r^{-\frac{b}{2}}(\varepsilon_0 - \varepsilon_{\infty}).\sin b\theta \tag{4}$$

Where:

$$r = \left[1 + (\omega\tau_0)^a.\cos\left(\frac{a.\pi}{2}\right)\right]^2 + \left[(\omega\tau_0)^a.\sin\left(\frac{a.\pi}{2}\right)^2\right] \tag{5}$$

$$\theta = arctg\left[\frac{(\omega\tau_0)^a.\sin\left(\frac{a.\pi}{2}\right)}{1 + (\omega\tau_0)^a.\cos\left(\frac{a.\pi}{2}\right)}\right] \tag{6}$$

As in the high-temperature region, the conductive process is dominant, in order to take into account the conductive contributions, we have included a new term in Eq. (2): $\varepsilon^*(\omega) = \varepsilon^*_{dip} + \varepsilon^*_{cond}$ with $\varepsilon^*_{cond}(\omega) = j(\sigma/e_0\omega)^s$ where e_0 is the free space dielectric permittivity (e_0 =8.854pF·m^{-1}), σ is the conductivity arising from charge transport at the liquid–electrode interface and s is a constant parameter with a value of one or close to one.

The HN and conductive fit parameters were determined at several temperatures from a multiple nonlinear regression analysis of the loss permittivity (ε'') experimental data, allowing the six characterizing processes parameters ($\Delta\varepsilon, \tau_0, a, b, \sigma/e_0, s$) to vary. For the isotherms analyzed only one dipolar relaxation contribution was considered and the b shape parameter was equal to one. Thus, equation 1 reduces to the Cole-Cole equation [38] that describes a relaxation with a relaxation times symmetric distribution. This result has been obtained for several heterogeneous systems [39-41], although for amorphous polymers a non-symmetric distribution of relaxation times (b< 1) is expected. The fit parameters obtained for the isotherms analyzed are summarized in Table 4 and plotted in Figures 7−8. An example of the deconvolution procedure is depicted in Figure 6 for the 223K isotherm.

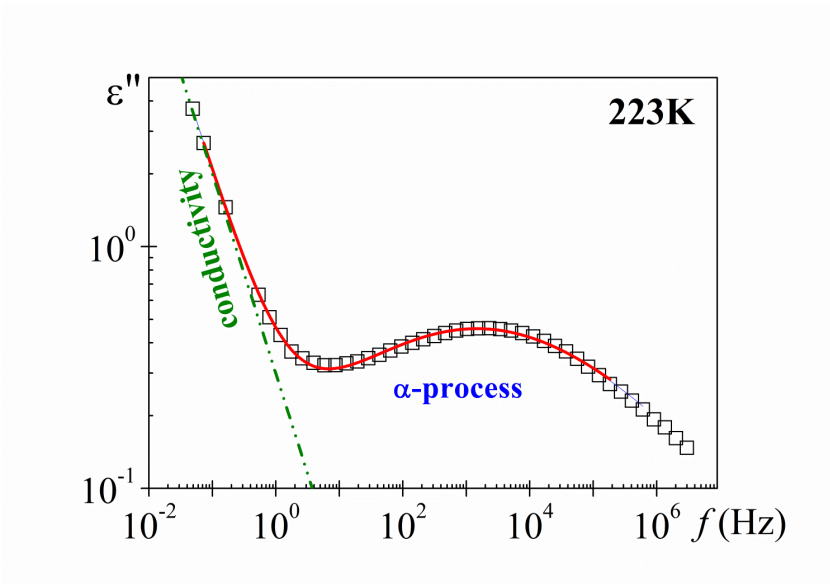

Figure 6 Frequency dependence of the loss permittivity of soybean oil polyol (SOP) samples at 223K, and its deconvolution of the conductive and α processes. Squares represent the experimental data, red line the global fit curve and blue and green lines represent the loss dielectric permittivity contribution of α and conductive processes, respectively.

Table 4 The HN and conductive fit parameters for soybean oil polyol (SOP) at several temperatures

between 208 and 248K.

T (K)	$\Delta\varepsilon$	f_{max} (Hz)	a	σ/e_0 (s^{-1})	s
208	3.98±0.05	$10^{0.85}\pm10^{0.27}$	0.27±0.01	0.05±0.01	0.88±0.01
213	3.97±0.035	$10^{1.72}\pm10^{0.30}$	0.27±0.01	0.15±0.01	0.87±0.01
218	3.96±0.06	$10^{2.48}\pm10^{0.43}$	0.28±0.02	0.48±0.02	0.85±0.02
223	3.94±0.05	$10^{3.18}\pm10^{0.49}$	0.29±0.01	1.37±0.01	0.83±0.01
228	3.92±0.10	$10^{3.79}\pm10^{0.71}$	0.30±0.02	3.65±0.05	0.86±0.01
233	3.90±0.21	$10^{4.31}\pm10^{0.83}$	0.31±0.02	9.08±0.14	0.88±0.01
238	3.87±0.16	$10^{4.74}\pm10^{0.85}$	0.33±0.02	19.60±0.24	0.88±0.01
243	3.87±0.11	$10^{5.13}\pm10^{0.87}$	0.34±0.01	44.33±0.72	0.92±0.01
248	3.83±0.26	$10^{5.49}\pm10^{0.98}$	0.36±0.02	89.37±1.81	0.94±0.01

The temperature dependence of the strength ($\Delta\varepsilon$) of the α process follows the classical trend, decreases with the temperature increasing because the molecular SOP structure is basically formed by fatty acids and flexible side chains few amounts with an amorphous structure highly disordered. The permanent dipoles orientation polarization decreases with temperature as the thermal energy disturbs the molecule dipoles alignment that contributes to the cooperative motions and gives rise to the relaxation [37]. Thus, the relaxation process in SOP presents different relaxation times because the friction between the dipole generates dielectric losses due to the dipole retardation to follow the frequency. As a result, the SOP mobility is reduced. As shown in Fig 7, the shape parameter *a*, related to the molecules freedom internal degrees increases as temperature increases indicating a decrease in the freedom internal degrees [42].

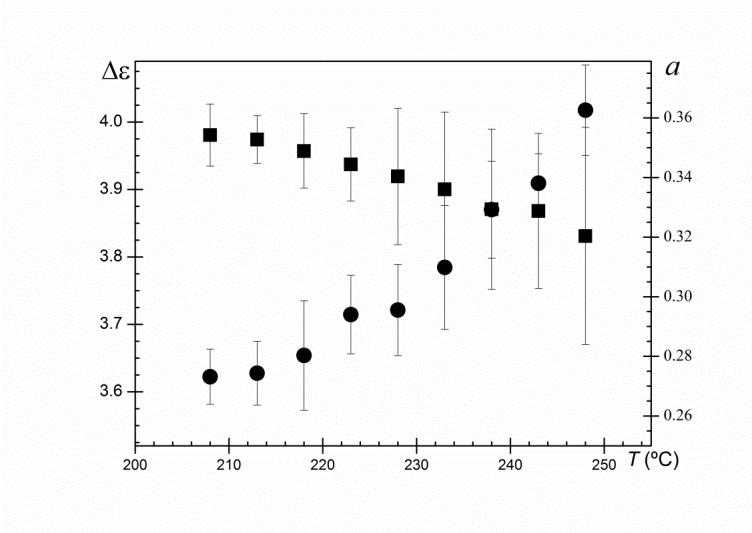

Figure 7 Temperature dependence of the dielectric strength (Δε) (square) and of the shape parameter (*a*) (circle) for soybean oil polyol (SOP). The shape parameter b was equal to unit for all analyzed isotherms.

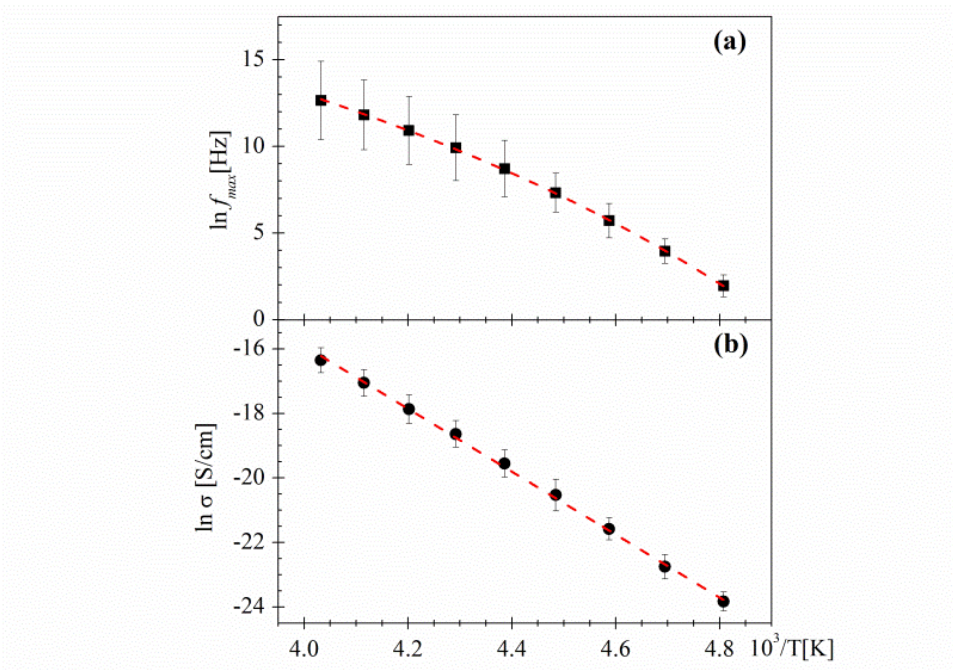

Figure 8 (a) Temperature dependence of ln f_{max} for α-relaxation process and (b) Temperature dependence of the conductivity, for soybean oil polyol (SOP).

The relaxation times temperature dependence for the α-relaxation process, associated with the peak maxima, is shown in Figure 8a. As usual for glass formers, the temperature dependence of the primary or α-relaxation is described by the Vogel-Fulcher-Tammann-Hesse (VFTH) Eq. 7 [43]:

$$\tau = \tau_0 \exp\left[-\frac{M}{T - T_v}\right] \tag{7}$$

where τ_0 is a pre-factor of the order of picoseconds, M is a material parameter defining its relaxation activation energy (energetic barrier to molecular rearrangement) and T_V, labeled as Vogel temperature, is the temperature at which τ extrapolates to infinity and the configurational entropy of the glassy system is nil. The VFTH fit parameters obtained by the fitting procedure were: M = (1722.78±122.91)K; ln τ_0= 29.55±0.82; T_v= (145.62±2.61)K. These parameters can be used to analyze the dynamic by means of: (i) the glass transition temperature (T_g) and (ii) the fragility or steepness index, m. The VFTH parameters enable us to extrapolate the data up to 100s and thereby to determine the glass transition temperature using the definition standard of T_g, i.e. $\tau_\alpha(T_g)$= 100s [44]. In this way, the SOP glass transition temperature evaluated from DRS measurements was equal to 193.48K (-79.52°C).

Another parameter to characterize the properties of glass-forming liquids, besides T_g, is the dynamic fragility index (m). This parameter can be determined by deviations from the Arrhenius temperature-dependence behavior of relaxation process (e.g., relaxation time, viscosity, fluidity), has

been widely used to investigate the macromolecular dynamics [45]. It can be evaluated from the slope at T_g of the curves in the Angell plot or by the M parameter of Eq. 8, as:

$$m = \frac{M}{2.303\, Tg \left(1 - \frac{T_v}{T_g}\right)^2} \tag{8}$$

The dynamic fragility index (m) is of particular interest for polymeric systems since it characterizes the change rate with which the properties of the system vary as the supercooled liquid temperature approaches its glass transition temperature [46]. Fragile liquids show a steeper increment in relaxation times approaching the glass transition than do strong liquids. Fragility values (dimensionless) typically range between m = 16, for strong systems, and m = 200 for the fragile ones [47]. According to the above definition of the dynamic fragility index, we have obtained the following value: 63.2±1.9. This value is similar to that one reported for other polyols [24]. On the other hand, the apparent activation energy associated with the chains relaxation dynamics at T_g can be obtained from the dynamic fragility index as $E_a\,(T_g) = 2.303\, R\, m\, T_g$. The value obtained was 234.1±6.9 kJ·mol^{-1}.

By comparing Eq. (7) with the Doolittle expression [48], the relative free volume at the glass temperature, $\phi_g/B = (T_g - T_v)/M$, and the thermal expansion coefficient of the free volume at T_g, $\alpha_f = 1/M$, can be evaluated. The relative free volume at the glass temperature, ϕ_g/B=2.78·10^{-2}±4.69·10^{-4}, and the free volume expansion coefficient, α_f = 5.80·10^{-4}±4.14·10^{-5} K^{-1}, evaluated are in agreement with those reported for other flexible polymers which lie in the vicinities of 2.5 × 10^{-2} ± 5.0 × 10^{-3} and (4−6) × 10^{-4} K^{-1}, respectively [49]. Finally, the temperature dependence of SOP the ionic conductivity, presented in Figure 7, obeys Arrhenius behavior with 81.07±0.94 kJ mol^{-1}activation energy.

DRS analysis contributed to the thermal behavior analysis since the T_g and the α-relaxation process, directly associated with conformational crankshaft motion characterized. Thus, SOP is a predominantly amorphous structure material and a fragile liquid. In general, renewable polyols have a high tendency to crystallize and are classified as fragile supercooled liquids [50]. In this way, the long chains with small pendant chains and the polar groups of the SOP molecular structure will have a pronounced effect on the polyurethane synthesis, reflecting on the fragility index decrease (soft segments α-relaxation in PUs) which indicates the increased flexibility [45].

4. CONCLUSIONS

In this paper, polyol soybean oil (SOP) was obtained by a microwave-assisted alcoholysis reaction. Studies of the reaction, thermal properties and relaxation processes of the SOP were

evaluated. The method we propose in this paper is an alternative to obtain SOP with short reaction times and without a catalyst. This is considered a scientific advance compared to previous research [4, 7, 16, 51]. Microwave-assisted alcoholysis proved to be a fast process to obtain SOP with good properties in just 5 min (300/20/10) s, without thermal degradation, besides energy savings and cleaner processes. On the other hand, for synthesis processes with 10 min reaction time, such as (600/40/05) s, and (600/50/01) s was enough to SOP degradation, resulting in a brown polyol. SOP (300/20/10) s showed 0.32 mg KOH·g^{-1}acid index, 150 mg KOH·g^{-1} saponification index, 190 mg KOH·g^{-1} hydroxyl number, 0.17 wt % water content, 1.463 g·mol^{-1} molecular weight, 4.98 average functionality, 2.4x10^{-5} mPa·s^{-1} viscosity at 333K and 1.00 g·cm^{-3} density. The method proposed by alcoholysis reaction resulted in high yields as 99.8 mol% opening and 98.5 mol% consumption of the epoxy ring. Employing the dielectric relaxation spectroscopy (DRS) for SOP was possible to identify α-relaxation process with a 193.5K glass transition (T_g), 63.2 fragility index and 234.1 kJ mol^{-1} activation energy associated with T_g from the dynamic fragility index. On the other hand, the ionic conductivity temperature dependence in SOP obeys Arrhenius behavior. $\Delta\varepsilon$ decreases with increased temperature due to the SOP amorphous structure, while a parameter indicated a decrease in the internal freedom degrees. The dielectric relaxation spectroscopy allowed the exact determination of the SOP's T_g, supporting the prediction of the microstructure (phase separation degree, micro phase composition and dynamic-mechanical properties) of the polyurethane to be synthesized. However, these properties are directly affected by the great influence of the nature of raw reagents such as SOP. This knowledge is essential not only from a scientific point of view but also for technological applications.

ACKNOWLEDGEMENTS

The authors thank the financial support from the Brazilian Agency Coordenação de Aperfeiçoamento de Pessoal de Nível Superior (CAPES) and Sindicato das Indústrias de Material Plástico do Nordeste Gaúcho (SIMPLÁS) for the gratification received at Jovens Pesquisadores 2017, da University of Caxias do Sul (UCS). CAF and OB are National Council for Scientific and Technological Development (CNPq) fellows. CMG and MJS thank the Spanish Ministerio de Economia y Competitividad (MAT2015-63955-R) for partial financial help. The authors also thank Dr. Cesar H. Wanke for the suggestions. This work was supported by CNPq-Brazil (06086/2018-2).

DECLARATIONS OF INTEREST

The authors declare that they do not have any conflict of interest.

DATA AVAILABILITY

Data not available / Data will be made available on request.

REFERENCES

[1] Ourique, P.A., Gril, J.M., Guillaume, G.W., Wanke, C.H., Echeverrigaray, S.G., Bianchi, O., 2015. Synthesis and characterization of the polyols by air oxidation of soybean oil and its effect on the morphology and dynamic mechanical properties of poly (vinyl chloride) blends. J. Appl. Polym. Sci. 132, e42102. https://doi.org/10.1002/app.42102.

[2] S. Allauddin, R. Narayan, K.V.S.N. Raju, Synthesis and properties of alkoxysilane castor oil and their polyurethane/urea–silica hybrid coating films, ACS Sustain. Chem. Eng. 8 (2013) 910−918. https://doi.org/10.1021/sc3001756.

[3] M. Clemente, R. Rocha, K. Iha, J. Rocco, Desenvolvimento de tecnologia de pré-polímeros na síntese de poliuretanos empregados em combustíveis sólidos, Quím. Nova. 37 (2014) 982−988. https://doi.org/10.5935/0100-4042.20140154.

[4] S. Dworakowska, D. Bogdal, A. Prociak, Microwave-assisted synthesis of polyols from rapeseed oil and properties of flexible polyurethane foams, Polymers. 4 (2012) 1462-1477. https://doi.org/10.3390/polym4031462.

[5] Roy, S.G., 2010. Novel approaches for synthesis of polyols from soy oils, PhD Dissertation, University of Toronto, Toronto, Canada, 61pp.

[6] M. Ionescu, Polyols from renewable resources - Oleochemical polyols, in: Chemistry and technology of polyols for polyurethanes, Rapra Technology Limited, United Kingdom, 2005, pp. 435−470.

[7] S. Allauddin, V. Somisetti, T. Ravinder, B.V.S.K. Rao, R. Narayan, K.V.S.N. Raju, One-pot synthesis and physicochemical properties of high functionality soy polyols and their polyurethane-urea coatings, Ind. Crops. Prod. 85 (2016) 361−371. https://doi.org/10.1016/j.indcrop.2015.12.087.

[8] I. Penso, E.A. Cechinatto, G. Machado, C. Luvison, C.H. Wanke, O. Bianchi, M.R. Soares, Preparation and characterization of polyhedral oligomeric silsesquioxane (POSS) using domestic microwave oven, J. Non Cryst. Solids. 428 (2015) 82−89. https://doi.org/10.1016/j.jnoncrysol.2015.08.020.

[9] A. Prociak, Rigid polyurethane foams modified with vegetable oil-based polyols, UTECH Europe Conference. Maastricht, paper, Nº. 39. 2006.

[10] P.A. B.Dariusz, A. Prociak, Renewable resources for the preparation of polymeric materials and polymer modification, in: Microwave-enhanced polymer chemistry and technology, Blackwell Publishing LTd., Poland, 2008, pp. 199-228.

[11] B. Lin, L. Yang, H. Dai, Q. Hou, L. Zhang, Thermal analysis of soybean oil based polyols, J. Therm. Anal. Calorim. 95 (2009) 977−983. https://doi.org/10.1007/s10973-007-8929-3.

[12] A.H. Willbourn, The glass transition in polymers with the $(CH_2)_n$ group, J. Chem. Soc. Faraday Trans. 54 (1958) 717−729. https://doi.org/10.1039/TF9585400717.

[13] Minoguchi, A., Kitai, K., Nozaki, R., 2003. Difference and similarity of dielectric relaxation processes among polyols. Phys. Rev. E. 68, e031501. https://doi.org/10.1103/PhysRevE.68.031501.

[14] I. Perepechko, Electrical properties of polymers at low temperature, in: Low-temperature properties of polymers, Pergamon Press, New York, 2013, pp.98-122.

[15] Lopes, R.d.V.V., 2015. Polyurethanes obtained from linseed oil (Linum usitatissimun L.) and passion fruit (Passiflora edulis Sims f. flavicarpa Degener). Unpublished M.Sc. Thesis, Universidade de Brasília, Brasília, 80pp.

[16] G. Acik, M. Kamaci, C. Altinkok, H.F. Karabulut, M.A. Tasdelen, Synthesis and properties of soybean oil-based biodegradable polyurethane films, Prog. Org. Coat. 123 (2018) 261−266. https://doi.org/10.1016/j.porgcoat.2018.07.020.

[17] E. Milchert, A. Smagowicz, The influence of reaction parameters on the epoxidation of rapeseed oil with peracetic acid, J. Am. Oil Chem. Soc. 86 (2009) 1227−1233. https://doi.org/10.1007/s11746-009-1455-7.

[18] ASTM, Standard D1639-90, Standard Test Method for Acid Value of Organic Coating Material, ASTM International, West Conshohocken, PA, (1990).

[19] ASTM, Standard D5558-95, Standard Test Method for Determination of the Saponification Value of Fats and Oils, ASTM International, West Conshohocken, PA, (1995).
[20] ASTM, Standard D4274-11, Standard Test Methods for Testing Polyurethane Raw Materials: Determination of Hydroxyl Numbers of Polyols, ASTM International, West Conshohocken, PA, (2011).
[21] ASTM, Standard E203-96, Standard Test Method for Water Using Volumetric Karl Fischer Titration, ASTM International, West Conshohocken, PA, (1996).
[22] P. Saithai, J. Lecomte, E. Dubreucq, V. Tanrattanakul, Effects of different epoxidation methods of soybean oil on the characteristics of acrylated epoxidized soybean oil-co-poly (methyl methacrylate) copolymer, Express. Polym. Lett. 7 (2013) 910−924. http://dx.doi.org/10.3144/expresspolymlett.2013.89.
[23] A. Campanella, J.J.L. Scala, R. Wool, Fatty acid-based comonomers as styrene replacements in soybean and castor oil-based thermosetting polymers, J. Appl. Polym. Sci. 119 (2011) 1000−1010. https://doi.org/10.1002/app.32810.
[24] C. Lebas, P. Turley, Primary hydroxyl content in polyols-evaluation of two nuclear magnetic resonance (NMR) methods, J Cell. Plast. 20 (1984) 194−199. https://doi.org/10.1177/0021955X8402000302.
[25] Cylindrical Liquid Sample Cell BDS 1307 Owner's Manual Issue: 6/2005 (c) 2005 by Novocontrol Technologies.
[26] C. Fu, Z. Yang, Z. Zheng, L. Shen, Properties of alkoxysilane castor oil synthesized via thiol-ene and its polyurethane/siloxane hybrid coating films, Prog. Org. Coat. 77 (2014) 1241−1248. https://doi.org/10.1016/j.porgcoat.2014.03.020.
[27] W. Xia, S.M. Budge, M.D. Lumsden, ^{1}H-NMR Characterization of epoxides derived from polyunsaturated fatty acids, J. Am. Oil Chem. Soc. 93 (2016) 467−478. https://doi.org/10.1007/s11746-016-2800-2.
[28] H.A. Aerts, P.A. Jacobs, Epoxide yield determination of oils and fatty acid methyl esters using ^{1}H NMR, J. Am. Oil Chem. Soc. 81 (2004) 841−846. https://doi.org/10.1007/s11746-004-0989-1.
[29] G.A. Oertel, Polyurethane Handbook: Chemistry, Raw materials, Processing, Application, properties, second ed., Hanser Publishers, New York, 1985.
[30] S. Mahajan, S.K. Konar, D.G. Boocock, Variables affecting the production of standard biodiesel, J. Am. Oil Chem. Soc. 84 (2007) 189−195. https://doi.org/10.1007/s11746-006-1023-3.
[31] Moraes, D.C.d., 2016. Síntese de polímeros oriundos do ácido oleico e derivados do biodiesel de soja e canola para revestimentos de nanopartículas de Fe_3O4 E $CoFe_2O_4$, Unpublished M.Sc. Thesis, Universidade Federal do Rio Grande do Sul, Rio Grande do Sul, Porto Alegre, 119pp. http://hdl.handle.net/10183/142123.
[32] Tuan Ismail, T.N.M., Palam, K.D.P., Bakar, Z.B.A., Soi, H.S., Kian, Y.S., Hassan, H.A., Schiffman, C., Sendijarevic, A., Sendijarevic, V., Sendijarevic, I., 2016. Urethane-forming reaction kinetics and catalysis of model palm olein polyols: quantified impact of primary and secondary hydroxyls. J. Appl. Polym. Sci. 133, e42955. https://doi.org/10.1002/app.42955.
[33] Ghoreishi, R., Zhao,Y., Suppes, G.J., 2014. Reaction modeling of urethane polyols using fraction primary secondary and hindered-secondary hydroxyl content. J. Appl. Polym. Sci. 131, e40388. https://doi.org/10.1002/app.40388.
[34] Z.S. Petrović, J. Milić, F. Zhang, J. Ilavsky, Fast-responding bio-based shape memory thermoplastic polyurethanes, Polymer. 121 (2017) 26−37. https://doi.org/10.1016/j.polymer.2017.05.072.
[35] T. Wang, J.L. Briggs, Rheological and thermal properties of soybean oils with modified FA compositions, J. Am. Oil Chem. Soc. 79 (2002) 831−836. https://doi.org/10.1007/s11746-002-0566-7.
[36] P.H.L. Pereira, 2010. Study of physical chemical properties of polyurethane derived from castor oil potential application in the medical. M. Sc. Dissertation, University of São Paulo, São Paulo, São Carlos, 120pp.
[37] Z. Shah, Q. Tahir, Dielectric properties of vegetable oils, Eur. J. Sci. Res. 3 (2011) 481−492. https://doi.org/10.3329/jsr.v3i3.7049.
[38] K.S. Cole, R.H. Cole, Dispersion and absorption in dielectrics I. Alternating current characteristics, J. Chem. Phys. 9 (1941) 341−351. https://doi.org/10.1063/1.1750906.
[39] B. Redondo-Foj, P. Ortiz-Serna, M. Carsí, M.J. Sanchis, M. Culebras, C.M. Gómez, A. Cantarero, Electrical conductivity properties of expanded graphite–polycarbonatediol polyurethane composites, Polym. Int. 64 (2015) 284−292. https://doi.org/10.1002/pi.4788.
[40] B. Redondo-Foj, M. Carsi, P. Ortiz-Serna, M. Sanchis, S. Vallejos, F. García, J. García, Effect of the dipole–dipole interactions in the molecular dynamics of poly (vinylpyrrolidone)-based copolymers, Macromolecules. 47 (2014) 5334−5346. https://doi.org/10.1021/ma500800a.
[41] P. Ortiz-Serna, R. Díaz-Calleja, M. Sanchis, E. Riande, R. Nunes, A. Martins, L. Visconte, Dielectric spectroscopy of natural rubber-cellulose II nanocomposites, J. Non Cryst. Solids. 357 (2011) 598−604. https://doi.org/10.1016/j.jnoncrysol.2010.06.044.

[42] T.S. Velayutham, W.A. Majid, A. Ahmad, G.Y. Kang, S. Gan, Synthesis and characterization of polyurethane coatings derived from polyols synthesized with glycerol, phthalic anhydride and oleic acid, Prog. Org. Coat. 66 (2009) 367−371. https://doi.org/10.1016/j.porgcoat.2009.08.013.
[43] H. Vogel, The law of the relation between the viscosity of liquids and the temperature, Phys. Z. 22 (1921) 645-646.
[44] A. Schönhals, F. Kremer, Broadband dielectric spectroscopy (e-Book), Springer, New York, 2003. https://doi.org/10.1007/978-3-642-56120-7.
[45] W. Yu, M. Du, D. Zhang, Y. Lin, Q. Zheng, Influence of dangling chains on molecular dynamics of polyurethanes, Macromolecules. 46 (2013) 7341−7351. https://doi.org/10.1021/ma401260d.
[46] D.J. Plazek, K.L. Ngai, Correlation of polymer segmental chain dynamics with temperature-dependent time-scale shifts, Macromolecules. 24 (1991) 1222−1224. https://doi.org/10.1021/ma00005a044.
[47] E.G. Merino, S. Atlas, M. Raihane, A. Belfkira, M. Lahcini, A. Hult, N. Dionísio, N.T. Correia, Molecular dynamics of poly (ATRIF) homopolymer and poly (AN-co-ATRIF) copolymer investigated by dielectric relaxation spectroscopy, Eur. Polym. J. 47 (2011) 1429−1446. https://doi.org/10.1016/j.eurpolymj.2011.04.006.
[48] A.K. Doolittle, Studies in Newtonian flow. I. The dependence of the viscosity of liquids on temperature, J. Appl. Phys. 22 (1951) 1031−1035. https://doi.org/10.1063/1.1700096.
[49] J.D. Ferry, Viscoelastic Properties of Polymers, third ed., John Wiley & Sons, New York, 1980.
[50] R.A. Talja, Y.H. Roos, Phase and state transition effects on dielectric, mechanical, and thermal properties of polyols, Thermochim. Acta. 380 (2001) 109−121. https://doi.org/10.1016/S0040-6031(01)00664-5.
[51] Pantone,V., Annese, C., Fusco, C., Fini, P., Nacci, A., Russo, A., D'Accolti, L., 2017. One-Pot Conversion of Epoxidized Soybean Oil (ESO) into Soy-Based Polyurethanes by $MoCl_2O_2$ Catalysis. Molecules. 22, e333. https://doi.org/10.3390/molecules22020333.

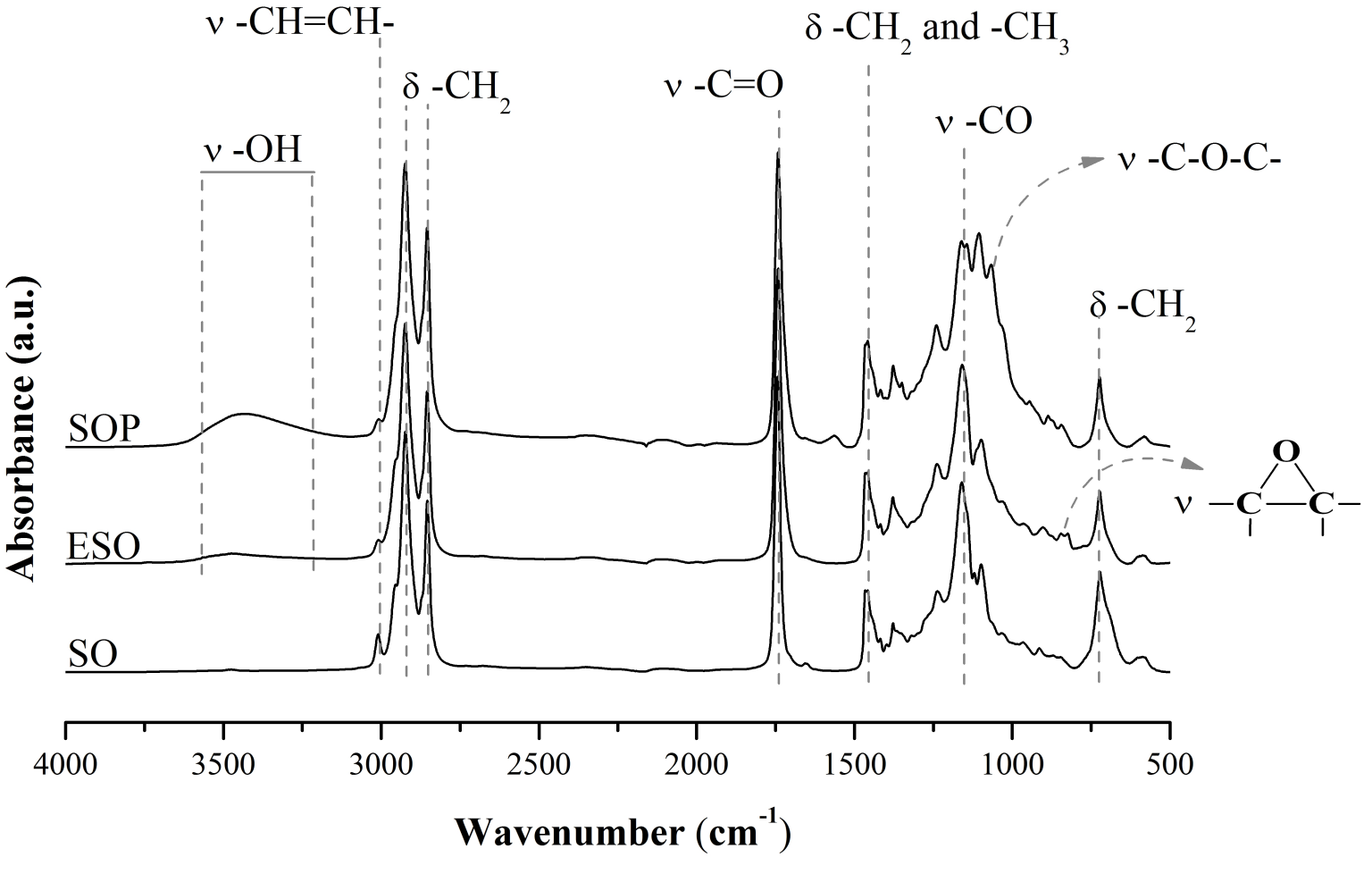
ν -CH=CH-
δ -CH2 and -CH3
δ -CH2
ν -C=O
ν -CO
ν -OH
ν -C-O-C-
δ -CH2
SOP
ESO
SO
ν
O
C
C
Absorbance (a.u.)
4000
3500
3000
2500
2000
1500
1000
500
Wavenumber (cm-1)

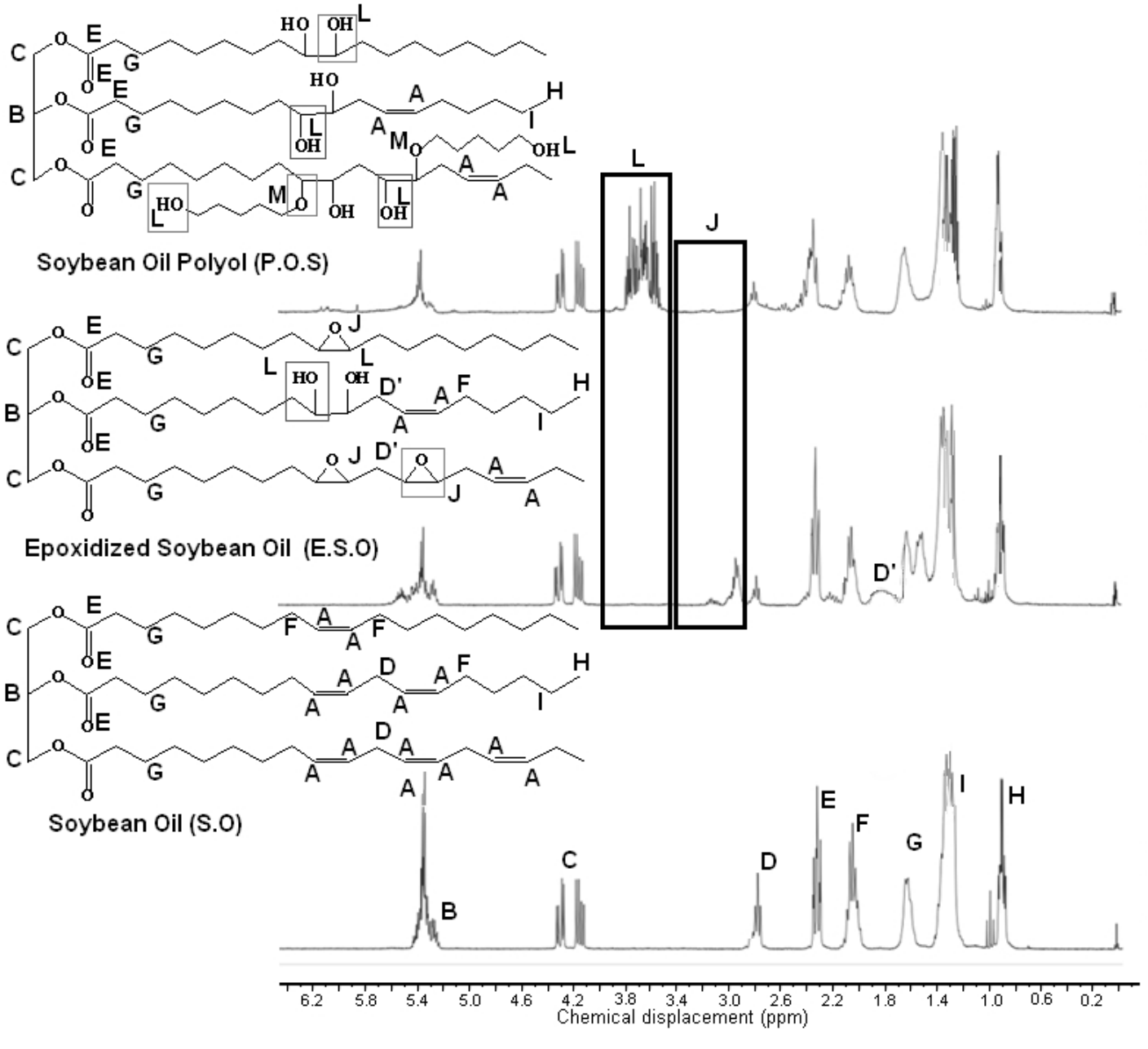
Soybean Oil Polyol (P.O.S)
Epoxidized Soybean Oil (E.S.O)
Soybean Oil (S.O)
Chemical displacement (ppm)
6.2
5.8
5.4
5.0
4.6
4.2
3.8
3.4
3.0
2.6
2.2
1.8
1.4
1.0
0.6
0.2

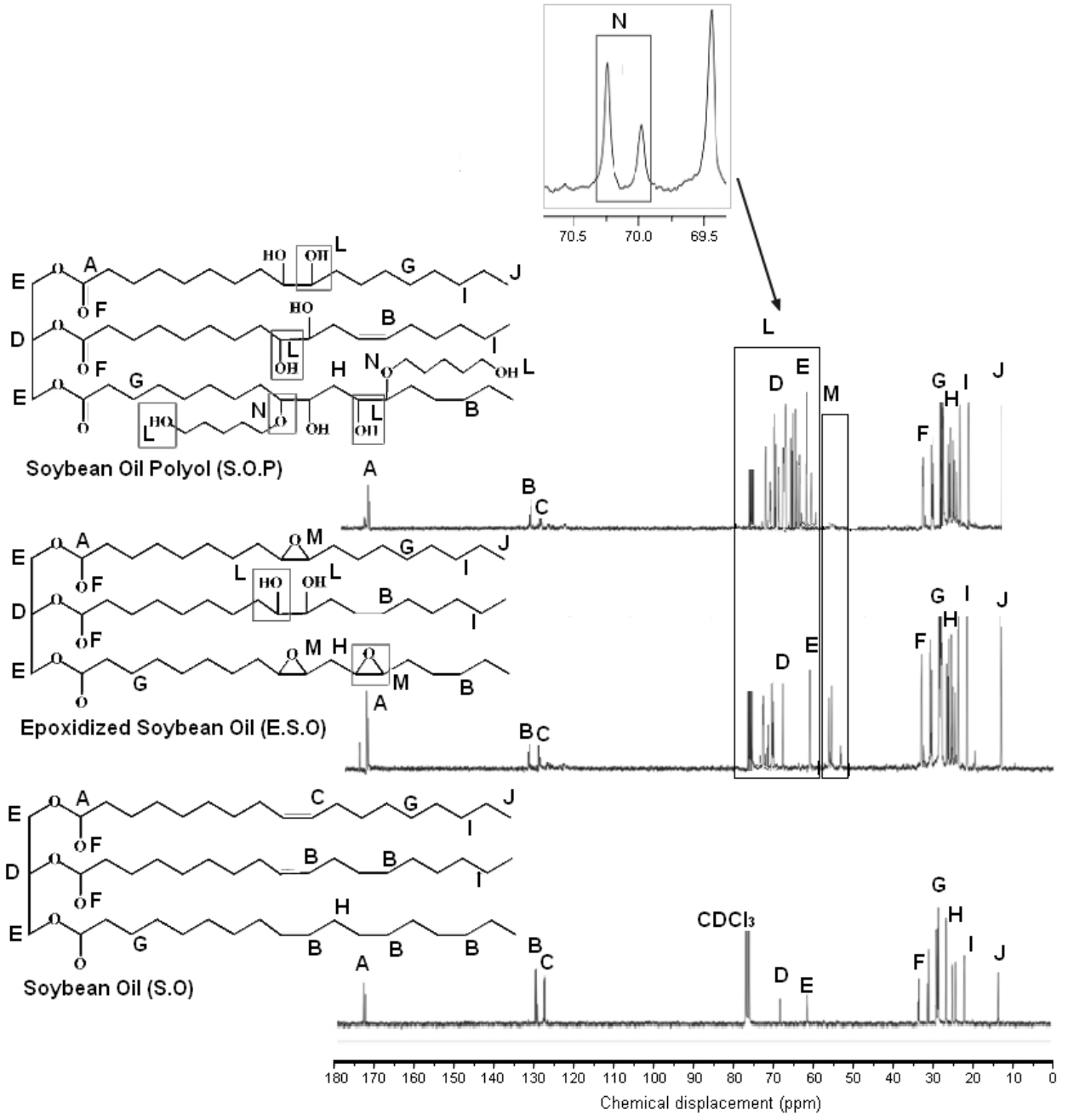
N
70.5
70.0
69.5
Soybean Oil Polyol (S.O.P)
Epoxidized Soybean Oil (E.S.O)
Soybean Oil (S.O)
CDCl3
180 170 160 150 140 130 120 110 100 90 80 70 60 50 40 30 20 10 0
Chemical displacement (ppm)

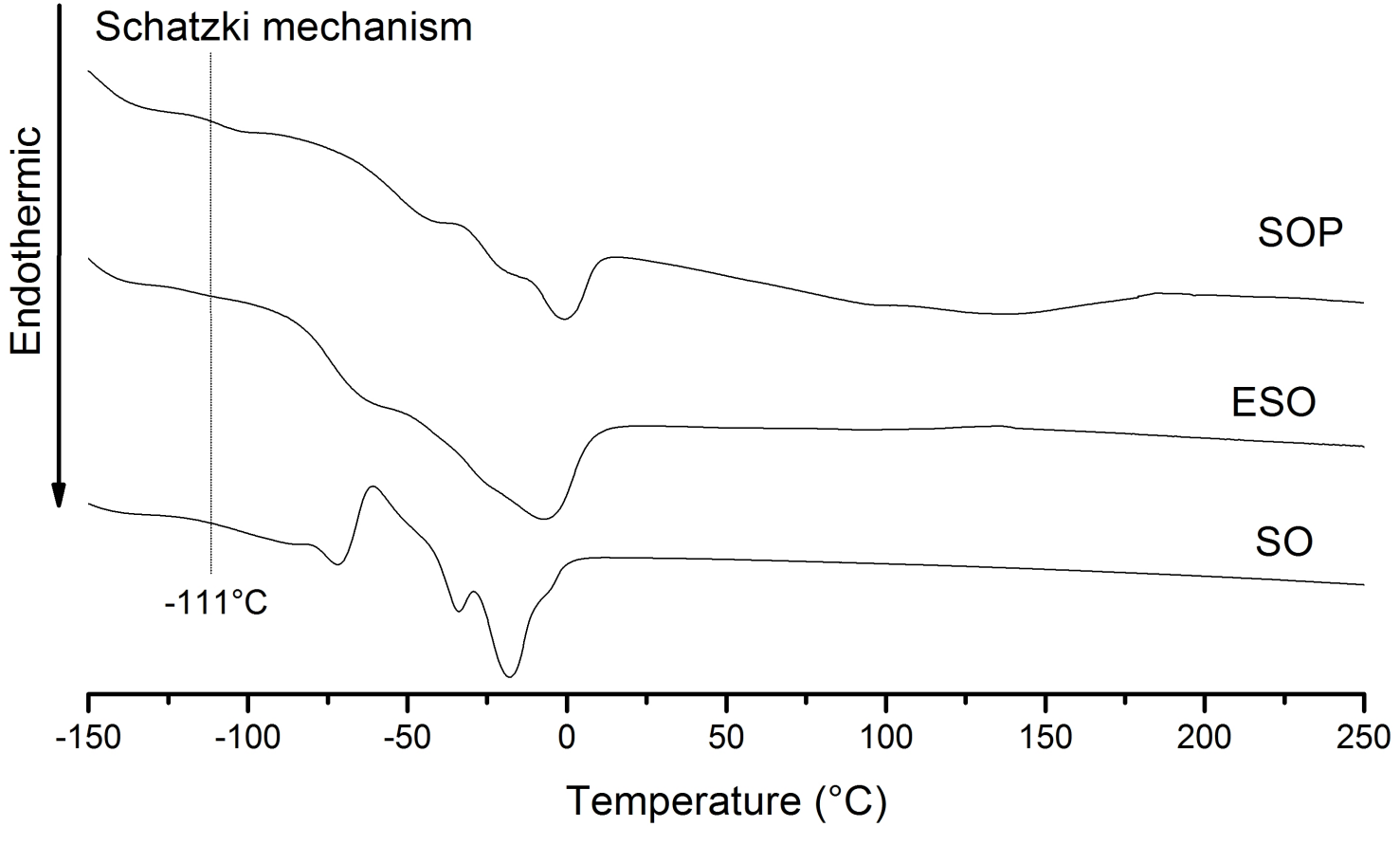
Schatzki mechanism
Endothermic
SOP
ESO
SO
-111°C
-150
-100
-50
0
50
100
150
200
250
Temperature (°C)

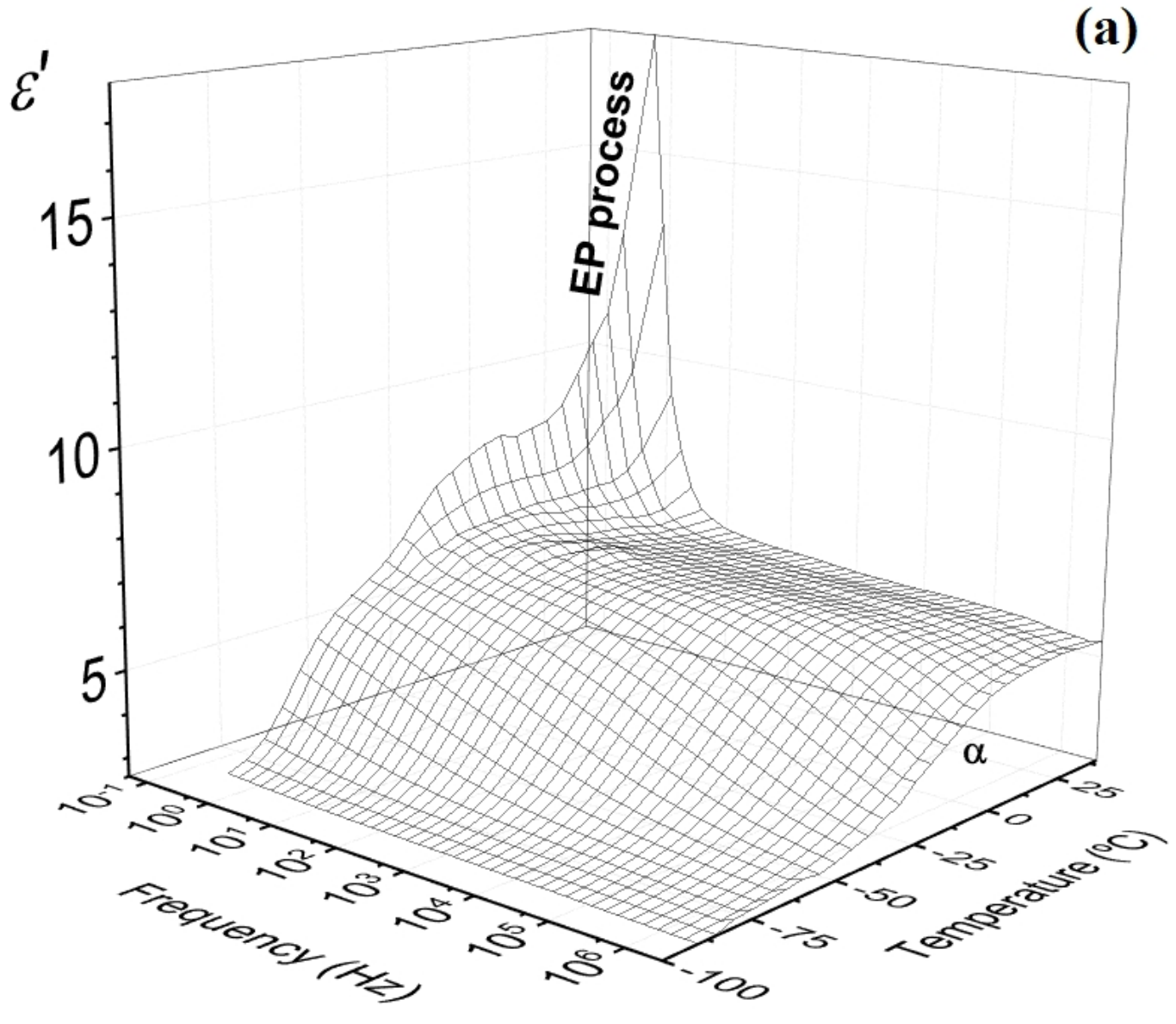
(a)
ε'
15
10
5
EP process
α
Frequency (Hz)
Temperature (°C)
25
0
-25
-50
-75
-100

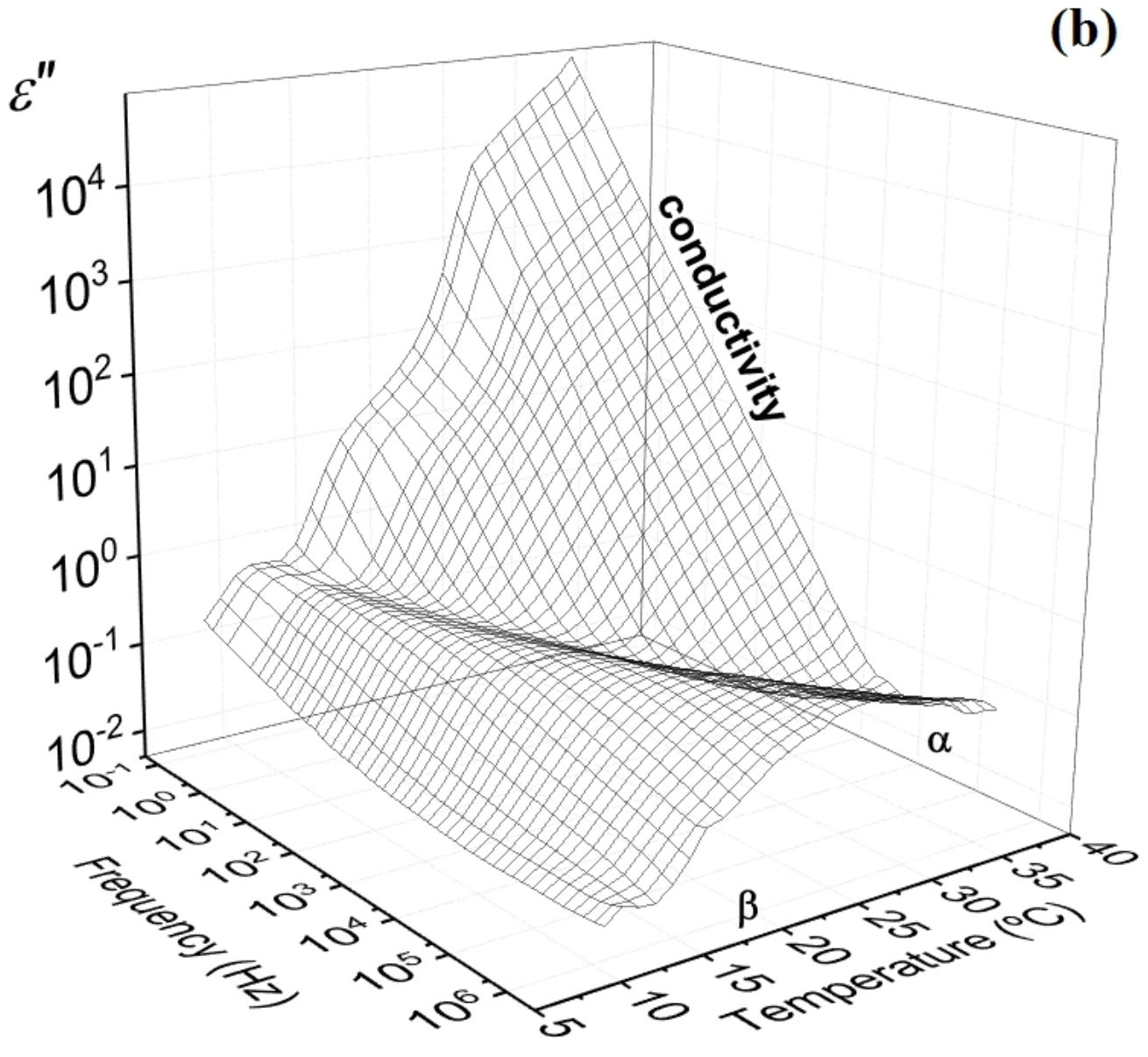
(b)
ε''
10^4
10^3
10^2
10^1
10^0
10^-1
10^-2
conductivity
α
β
10^-1
10^0
10^1
10^2
10^3
10^4
10^5
10^6
Frequency (Hz)
5
10
15
20
25
30
35
40
Temperature (°C)

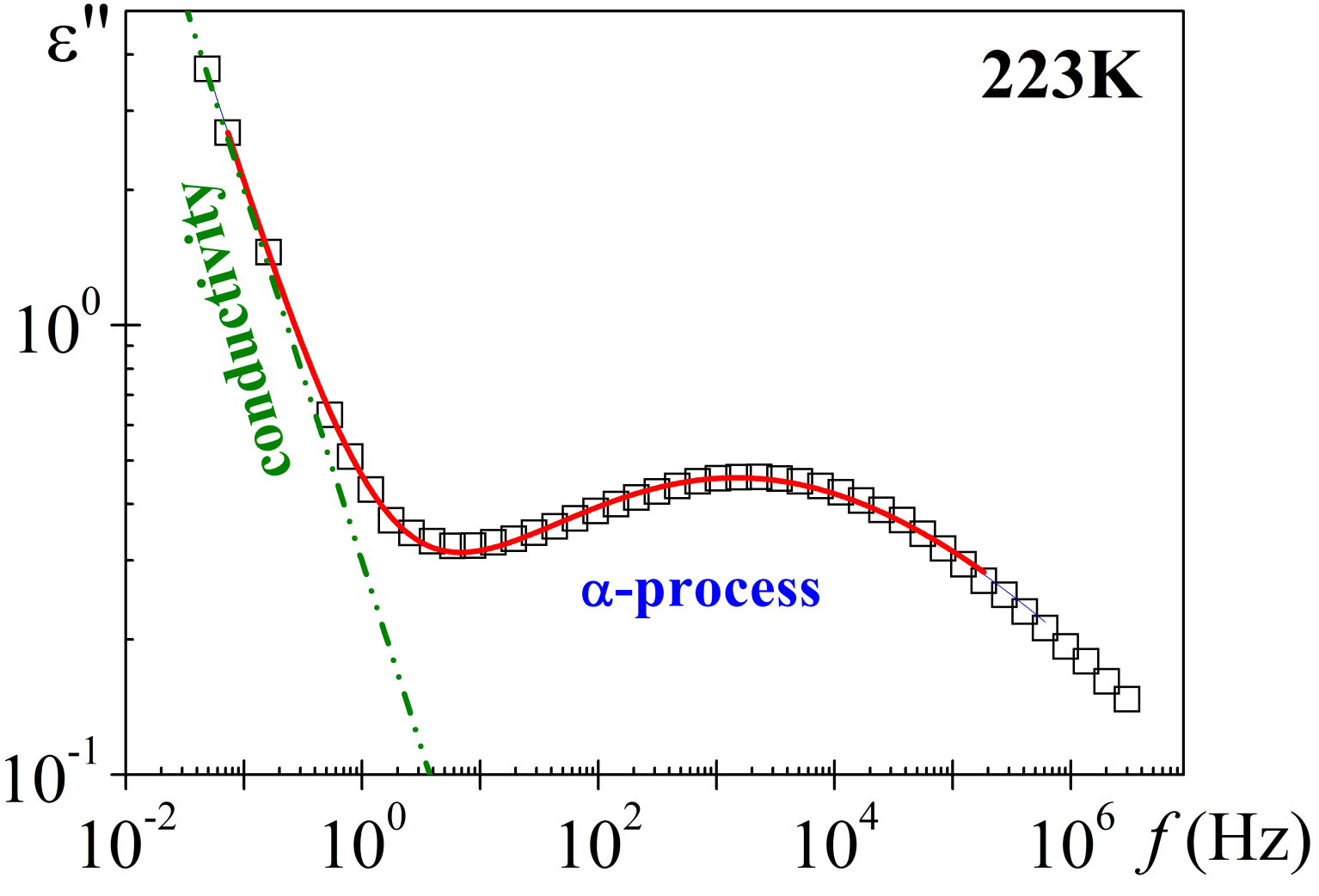
ε''
223K
conductivity
α-process
10^0
10^{-1}
10^{-2}
10^0
10^2
10^4
10^6
f (Hz)

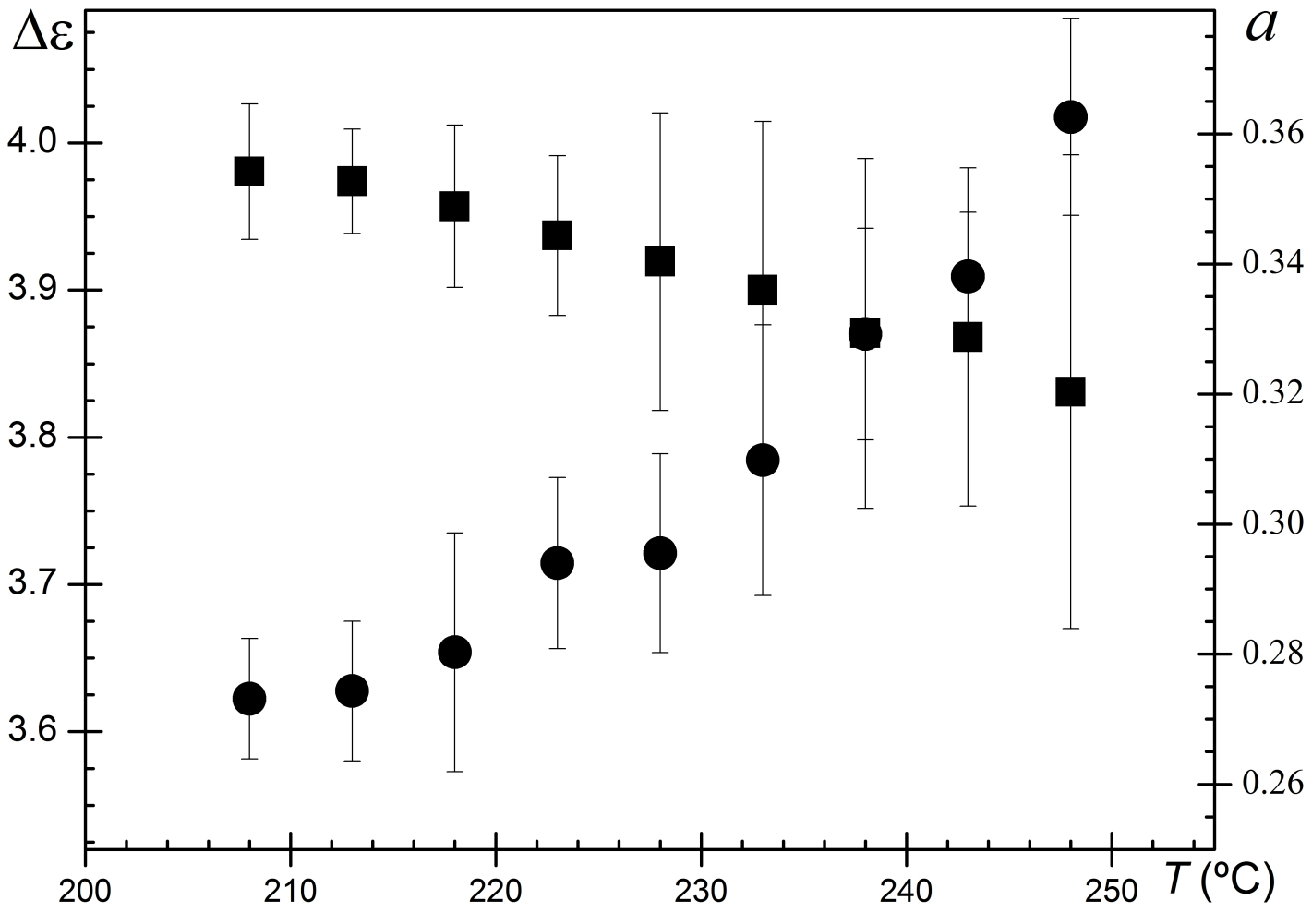
Δε
a
4.0
3.9
3.8
3.7
3.6
0.36
0.34
0.32
0.30
0.28
0.26
200
210
220
230
240
250
T (ºC)

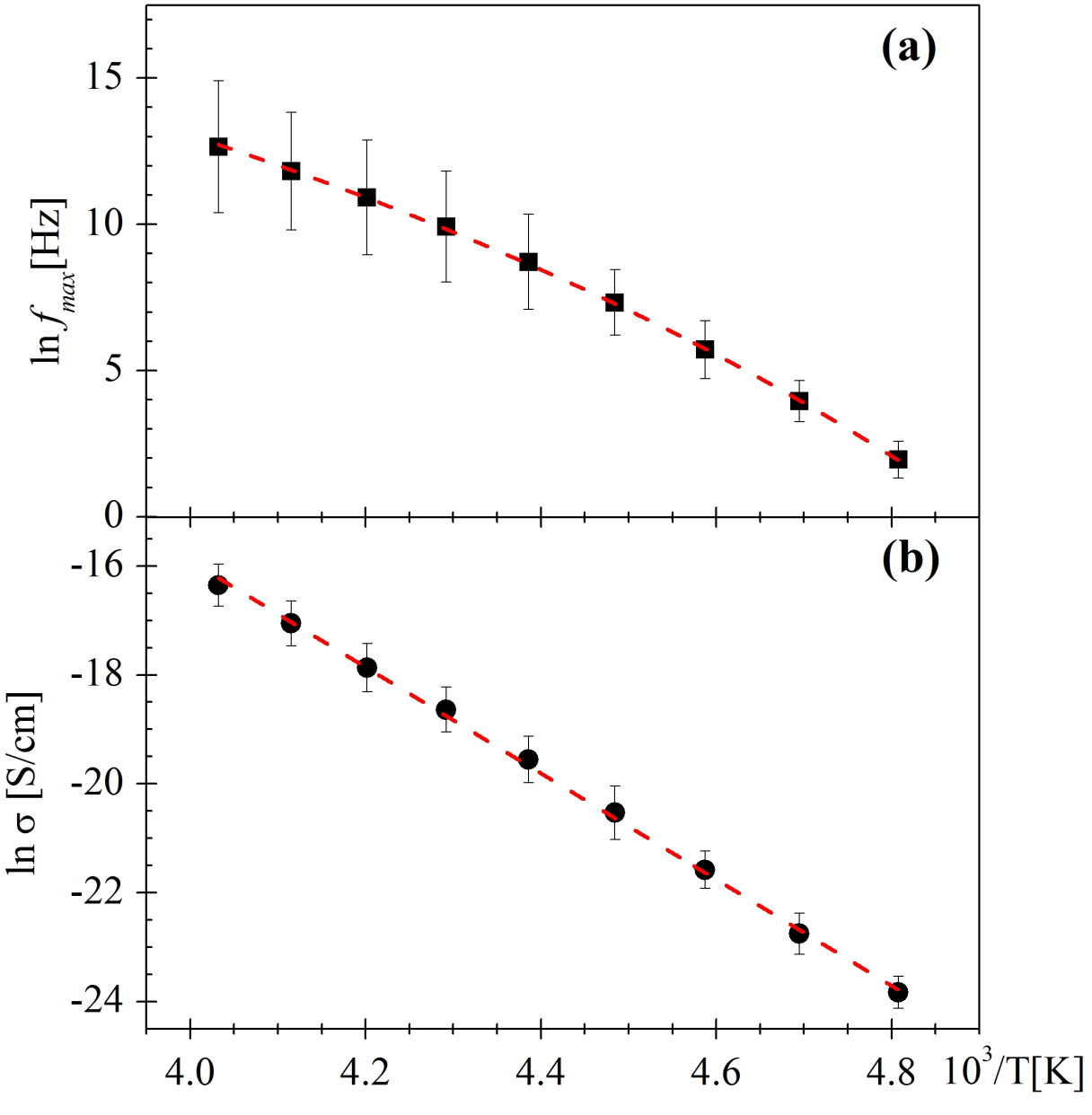
(a)
(b)
ln f_{max} [Hz]
ln σ [S/cm]
15
10
5
0
-16
-18
-20
-22
-24
4.0
4.2
4.4
4.6
4.8
10^3/T[K]

Table 1 Titrations, GPC, density and viscosity analysis of the soybean oil (SO), epoxidized soybean oil (ESO) and soybean oil poliol (SOP)

Properties	SO*	ESO	SOP
Acid index (mg KOH·g^{-1})	0.80	28.70	0.32
Saponification index (mg KOH·g^{-1})	146	149	150
Hydroxyl number (mg KOH·g^{-1})	0.20	53	190
Water content (wt %)	—	—	0.17
Density (g·cm^{-3})	0.90	0.97	1.00
Molecular weight (g·mol^{-1})	936	1125	1463
Average functionality (OH)	-	1.12	4.98
Viscosity at 333K (mPa·s^{-1})	1.7x10^{-6}	1.9x10^{-6}	2.4x10^{-5}

Table 2 Yield of soybean oil polyol (SOP) by ^{1}H NMR analysis. The opening (ER) and consumption (E) of the epoxide ring

Samples Time/pulse on/off (s)	ER (mol%)	E (mol%)
300/20/10	99.8 ±0.1	98.5 ±0.1
300/40/05	90.1±0.3	43.2±0.1
300/50/01	89.0±0.4	43.1±0.2
600/20/05	86.0±0.1	46.6±0.4
600/20/10	86.0± 0.1	46.6± 0.3
600/40/05	84.4±0.5	46.7±0.1
600/50/01	81.9±0.1	44.3±0.3

Table 3 Properties to epoxidized soybean oil (ESO) and soybean oil polyol (SOP) by H^1 and ^{13}C NMR spectra quantification

Properties (mol%)	ESO	SOP
Primary hydroxyl groups (X_P)	37.1 ± 1.1	65.8 ± 1.5
Secondary hydroxyl groups (X_s)	62.9 ± 0.9	34.2 ± 1.2
Epoxidation degree (EG)	60.2 ± 0.5	—
Epoxy ring number for TGD (E)	2.73 ± 0.4	—
Double bonds consumption (DC)	66.1 ± 1.2	70.5 ± 1.6
Selectivity (S)	—	71.6 ± 0.3

Table 4 The HN and conductive fit parameters for soybean oil polyol (SOP) at several temperatures between 208 and 248K

***T*, K**	$\Delta\varepsilon$	f_{max} *(Hz)*	*a*	σ/e_0 (s^{-1})	*s*
208	3.98±0.05	$10^{0.85}\pm10^{0.27}$	0.27±0.01	0.05±0.01	0.88±0.01
213	3.97±0.035	$10^{1.72}\pm10^{0.30}$	0.27±0.01	0.15±0.01	0.87±0.01
218	3.96±0.06	$10^{2.48}\pm10^{0.43}$	0.28±0.02	0.48±0.02	0.85±0.02
223	3.94±0.05	$10^{3.18}\pm10^{0.49}$	0.29±0.01	1.37±0.01	0.83±0.01
228	3.92±0.10	$10^{3.79}\pm10^{0.71}$	0.30±0.02	3.65±0.05	0.86±0.01
233	3.90±0.21	$10^{4.31}\pm10^{0.83}$	0.31±0.02	9.08±0.14	0.88±0.01
238	3.87±0.16	$10^{4.74}\pm10^{0.85}$	0.33±0.02	19.60±0.24	0.88±0.01
243	3.87±0.11	$10^{5.13}\pm10^{0.87}$	0.34±0.01	44.33±0.72	0.92±0.01
248	3.83±0.26	$10^{5.49}\pm10^{0.98}$	0.36±0.02	89.37±1.81	0.94±0.01

Supplementary files

Supplementary Table

Table S1 ^{1}H NMR chemical shifts observed from the reaction of epoxidation and alcoholysis of soybean oil [27]:

Spectrum [a]	Signal	Chemical shift (ppm)	Protons	Functional groups/ coupling constant (J)
SO	A e B	5.20-5.55 (m)	-C**H**=C**H-**	olefinic group
	C	4.10 – 4.35 (dd)	CH -C**H$_2$**-C=O-O-	hydrogens directly attached to the glycerol portion/ ^{3}J = 4,2 Hz
	D	2.8 (t)	-CH=CH-C**H$_2$**-CH=CH-	diallylic methylene group / ^{3}J = 5,7 and ^{3}J = 6,3 Hz
	E	2.16 (m)	-CH$_2$- C**H$_2$**—CH=CH-	allylic methylene group
	F	2.0 (t)	CH$_2$-C**H$_2$**-C=O-O-	methylene group alpha to acyl group / ^{2}J = 6,4 Hz
	G	1.5 (m)	C**H$_2$**-CH$_2$-C=O-O-	methylene group beta to acyl group
	H	0.88 (t)	C**H$_3$**-CH$_2$-CH$_2$-	terminal methyl group / ^{1}J=2,7
ESO	A’	5.50-5.60 (m)	-CH△CH-CH$_2$-CH=C**H-**	olefinic group beta to epoxy group
	B’	5.35-5.5 (m)	-CH△CH-CH$_2$-C**H**=CH-	
	F’	2.0 (m)	-CH△CH-C**H$_2$**-CH△CH-	methylene group between two epoxy groups
	J’	2.90-3.00 (m)	-C**H**△CH-CH$_2$-CH△C**H-**	epoxy groups separated by a methylene group
	J’’	3.01-3.14 (m)	-CH△C**H**-CH$_2$-C**H**△CH-	
	D’	1.61 (m)	-CH$_2$-C**H$_2$** -CH △CH-	methylene group alpha to epoxy group
	G’	1.45 (m)		
	H’	0.88 (t)	C**H$_3$**-CH$_2$-CH$_2$-	terminal methyl group / ^{1}J=2,7
SOP		3.40 (m)	-CH$_2$-C**H**(OH)-C**H**(OH)- CH$_2$-	beta methine group to hydroxyl groups
	L	3.54 (m)	-CH$_2$-(O-CH$_2$-CH$_2$-O-C**H$_2$**-CH$_2$-OH)	alpha methylene group to hydroxyl group
		3,54-3,76 (m)	OH-CH$_2$-CH$_2$-O**H**	methylene hydrogens bonded to hydroxyl groups

(t) triplet, (m) multiplet, (dd) dublete dublete [27];
[a] Here, soybean oil (SO), epoxidized soybean oil (ESO) and soybean oil polyol (SOP) corresponded to the ^{1}H NMR in Figure 2.

Table S2 ^{13}C NMR chemical shifts observed from the reaction of epoxidation and alcoholysis of soybean oil:

Spectrum [a]	Signal	Chemical shift (ppm)	Protons	Functional Groups/ coupling constant (J)
SO	B - C	127-130 (m)	-H**C**=**C**H-	olefinic group
	D	68.87 (m)	-H_2**C**-O-CO-	methylene group alpha to group acyl
	E	61.1(m)	-H**C**-O-CO-	methino group alpha to group acyl
	G	22-34 (m)	-CH_2-**C**H_2-CH_2-CH_3	methylene group betha to terminal methyl group
	F		-CH_2-**C**H_2-C=O-O-CH_3	methylene group alpha to acyl group
	H		-**C**H_2-CH_2-CO-O-CH_3	methylene group betha to acyl group
	I		-CH_2-CH_2-**C**H_2-CH_3	methylene group alpha to terminal methyl group
	J	13.5 (s)	CH_2-CH_2-**C**H_3-	terminal methyl group
	A	173.0 (m)	-H_2C-O-**C**O-	carbon from carboxyl group
ESO	M	60.9	-H**C**△**C**H-CH_2-CH=CH-	epoxy group beta to oleofinic group
	H	25,8 (m)	-CH_2-△-**C**H_2-△CH_2-	methylene group between two epoxy groups
	G	22.0-34.0 (m)	-**C**H_2-CH_2-CH_2-CH(OH)-CH_2-	methylene group gamma to hydroxyl group
	H		-CH_2-**C**H_2-CH_2-CH(OH)-CH_2-	methylene group betha to hydroxyl group
SOP		60.0-61.1	-HC(O- **C**H_2-CH_2-O-**C**H_2-CH_2-OH)	methylene group alpha to ether group
	L	60.2-65.8	-CH_2-**C**H_2(OH)-CH_2	methylene group alpha to primary hydroxyl group
		65.9-89.9	-C(O-CH_2-CH_2-O-CH_2-**C**H_2-OH)	methylene group alpha to secondary hydroxyl group

(t) triplet, (m) multiplet, (dd) dublete dublete [27];
[a] Here, soybean oil (SO), epoxidized soybean oil (ESO) and soybean oil polyol (SOP) corresponded to the ^{13}C NMR in Figure 3.